

Long-range photon fluctuations enhance photon-mediated electron pairing and superconductivity

Ahana Chakraborty¹ and Francesco Piazza¹

¹Max Planck Institute for the Physics of Complex Systems, Nöthnitzer Str. 38, 01187, Dresden, Germany.

(Dated: November 15, 2021)

Recently, the possibility of inducing superconductivity for electrons in two dimensional materials has been proposed via cavity-mediated pairing. The cavity-mediated electron-electron interactions are long range, which has two main effects: firstly, within the standard BCS-type pairing mediated by adiabatic photons, the superconducting critical temperature depends polynomially on the coupling strength, instead of the exponential dependence characterizing the phonon-mediated pairing; secondly, as we show here, the effect of photon fluctuations is significantly enhanced. These mediate novel non-BCS-type pairing processes, via non-adiabatic photons, which are not sensitive to the electron occupation but rather to the electron dispersion and lifetime at the Fermi surface. Therefore, while the leading temperature dependence of BCS pairing comes from the smoothening of the Fermi-Dirac distribution, the temperature dependence of the fluctuation-induced pairing comes from the electron lifetime. For realistic parameters, also including cavity loss, this results into a critical temperature which can be more than one order of magnitude larger than the BCS prediction. Moreover, a finite average number photons (as can be achieved by incoherently pumping the cavity) adds to the fluctuations and leads to a further enhancement of the critical temperature.

Introduction. The development of experimental solid state platforms coupling electrons with the quantum light of optical cavities [1, 2] offers exciting prospects for the exploration of novel types of collective phenomena, which can arise due to the peculiar nature of the cavity-mediated interactions and their interplay with electronic correlations. Several scenarios have been theoretically investigated, with relevance for solid-state materials [3–11] and ultracold fermionic atoms [12–22].

One particular direction which is receiving considerable attention is the possibility to induce electronic superconductivity via photon-mediated pairing [7, 9]. The critical temperature has been predicted to follow a non-exponential dependence on the light-matter coupling strength, which can be explained within the usual BCS paradigm as due to the long-range character of the cavity-mediated interactions i.e. the fact that the photons transfer a well defined momentum.

In this letter, we show that the long-range nature of the cavity-mediated interactions can have an even more dramatic influence on superconductivity, which is to introduce a novel, non-BCS-type of pairing mediated by on-shell, non-adiabatic photon fluctuations. This is different from BCS pairing, which involves instead the emission/absorption of adiabatic, off-shell photons, and depends on the thermal occupation of electrons. On the other hand, the fluctuation-mediated pairing is only directly affected by the electron dispersion and lifetime near the Fermi surface. Therefore, temperature hinders this non-BCS-type of pairing by decreasing the electron lifetime, while it affects the BCS pairing mainly by smoothening the Fermi-Dirac distribution.

This new fluctuation-mediated pairing can enhance superconductivity significantly. Considering a Fermi-liquid-type electron lifetime set by the screened Coulomb interaction, the critical temperature can be more than one order of magnitude larger than the BCS prediction, using realistic parameters for the terahertz cavities considered in Ref.[9] and including photon loss.

At the typical transition temperatures, optical cavities are

unoccupied on average, such that only vacuum fluctuations or loss-induced noise contribute to the non-BCS-type pairing. A finite average number of photons can be achieved by pumping the cavity, which then further amplifies this type of pairing. In this way, the critical temperature can be enhanced at least until the Fermi-liquid picture holds, approaching thus the Fermi-temperature (slightly above 10 K for the materials considered in Ref.[9]), even at moderate electron-photon coupling.

Model. We consider a 2D electron system coupled to a terahertz cavity. The phenomenology discussed here relies on two properties of the cavity field. The first and most important feature is that the cavity-mediated interaction is long ranged. We model this by restricting the momentum transferred by the photon to a fixed vector \vec{q}_0 . This simplest model corresponds to the case of a split-ring cavity [9], sustaining a standing-wave mode of frequency ω_c , and momentum $\pm q_0 \hat{x}$, with $q_0 = \omega_c \sqrt{\epsilon_r}/c$. Here, ϵ_r is the relative permittivity of the 2D material and c is speed of light in vacuum. We shall show that our results remain essentially unchanged in the limit $q_0 \rightarrow 0$ as well as by allowing for a broadening of the photon momentum, provided the corresponding frequency width is smaller than the electron lifetime at the Fermi surface (FS). This extends the applicability of our results to the case of the planar microcavity geometry considered in Ref.[7], where the set of propagating transverse modes is distributed around $q = 0$ with a narrow width set by ω_c/c , where now ω_c is the frequency of the purely longitudinal mode. The second feature we consider here is that the cavity field couples to the electron density. As shown in Ref.[9], this can be achieved by driving the system with a transverse laser beam of frequency ω_L which is detuned from the cavity frequency by $\delta_c = \omega_c - \omega_L$. For sufficiently strong laser driving, the dominant light-matter interaction is induced via two-photon diamagnetic processes [9] and reads

$$H_{\text{light-matter}} = \sum_{\vec{k}, \sigma} \sum_{\vec{q}=\pm q_0 \hat{x}} g_0 c_{\vec{k}+\vec{q}, \sigma}^\dagger c_{\vec{k}, \sigma} (b + b^\dagger), \quad (1)$$

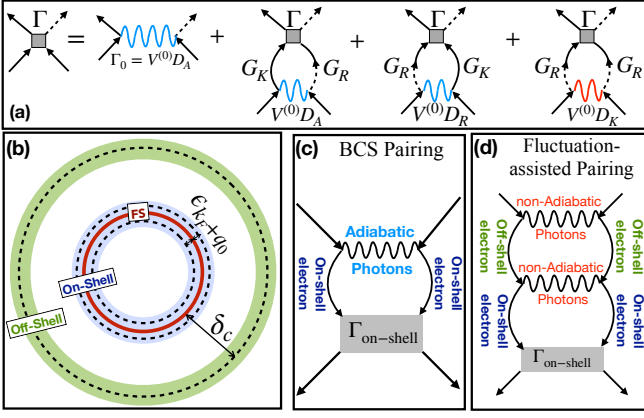


FIG. 1. (a) The real-time Keldysh formulation of the Bethe-Salpeter equation for the vertex function Γ in the pairing channel. It contains the bare vertex Γ_0 (1st diagram), the standard BCS terms Γ_{BCS} (2nd and 3rd diagrams), and the “fluctuation term”, Γ_{fluct} (4th diagram). The latter leads to a non-BCS-type of pairing. (b) The electronic energy structure can be divided between on-shell electrons in the vicinity of the FS: $\omega_1 \sim \epsilon_{k_F \pm q_0}$ and off-shell electrons excited to photonic frequencies: $\omega_1 \sim \delta_c$ (see eq. (3)). (c) Standard BCS pairing: the scattering via off-shell adiabatic photons leaves the electrons on-shell. (d) Fluctuation-induced pairing: on-shell non-adiabatic photons at frequencies $\pm \delta_c$ induce pairing between on-shell electrons through an intermediate transition to off-shell electronic states.

where b^\dagger and $c_{\vec{k},\sigma}^\dagger$ are the creation operator of cavity photons of momentum \vec{q}_0 and electrons of momentum \vec{k} and spin σ respectively. The coupling strength g_0 is tuneable by the intensity of the external laser beam.

Causal structure of the pairing. We compute the superconducting critical temperature T_c via the pairing instability of the vertex function Γ in the Cooper pairing channel, involving electrons moving with opposite momenta \vec{p} and $-\vec{p}$. The Dyson equation for the vertex function is known as the Bethe-Salpeter (BS) equation [23], which we formulate using real-time Green’s functions (GFs) defined on the Keldysh closed time-contour. Besides being suited to include cavity loss (and incoherent pumping), this approach also allows to clearly separate the non-BCS-type, fluctuation-induced pairing we propose here from the standard BCS pairing. The BS equation in its simplest form has the following structure (see Fig. 1(a) and Appendix B [24]),

$$\Gamma = \Gamma_0 + \Gamma_{\text{BCS}} + \Gamma_{\text{fluct}} \quad (2)$$

where $\Gamma_0 = V^{(0)}D_A$ is the bare vertex. Here $\Gamma(\vec{p}, \omega)$ is a function of the relative momentum and frequency of the incoming electrons. Within the ladder approximation [23, 25] for the vertex function we have,

$$\begin{aligned} \Gamma_{\text{BCS}}^{A(R)}(p) &= \mathbf{i} \int_k V^{(0)}D_{A(R)}(k-p) G_{K(R)}(k) G_{R(K)}(-k) \Gamma(k) \\ \Gamma_{\text{fluct}}(p) &= \mathbf{i} \int_k V^{(0)}D_K(k-p) G_R(k) G_R(-k) \Gamma(k), \end{aligned} \quad (3)$$

with the coupling function $V^{(0)}(\vec{k} - \vec{p}) = g_0^2 \delta_c \delta_{\vec{k}-\vec{p}, \pm q_0 \hat{x}}$. Here, $p = (\vec{p}, \omega)$, $k = (\vec{k}, \omega_1)$ and $\int_k = \int d\vec{k} d\omega_1 / (2\pi)^3$. We denote here the electron and photon GFs by G and D , respectively. Within the real-frequency Keldysh formulation, each GF can be of two types: a retarded (advanced) GF (denoted by the subscript $R(A)$) or a Keldysh GF (denoted by the subscript K).

Formulated in momentum-frequency space, the retarded GF contains only information about the dispersion and lifetime of the (quasi)particles, while the Keldysh component explicitly depends also on the occupation of the quasiparticle modes. In thermal equilibrium, these two Green’s functions are connected by a Fluctuation-Dissipation relation [26]. We first consider a situation where the whole system is at temperature T , and the GFs entering the BS equation read [26] (see appendix A [24]),

$$\begin{aligned} G_{R(A)}(\vec{k}, \omega) &= \frac{1}{\omega - \epsilon_k \pm \mathbf{i}0^+}, \\ G_K(\vec{k}, \omega) &= -2\pi \mathbf{i} \tanh\left(\frac{\omega}{2T}\right) \delta(\omega - \epsilon_k), \\ D_{R(A)}(\omega) &= \frac{1}{2} \frac{1}{(\omega \pm \mathbf{i}0^+)^2 - \delta_c^2}, \\ D_K(\omega) &= \frac{-\pi \mathbf{i}}{2\delta_c} [\delta(\omega - \delta_c) - \delta(\omega + \delta_c)] \coth\left(\frac{\omega}{2T}\right). \end{aligned} \quad (4)$$

Here, ϵ_k is the dispersion of the electrons measured from the Fermi energy, E_F . Let us now discuss the physical interpretation of the terms contributing to the BS equation (2). The standard BCS term $\Gamma_{\text{BCS}} = \Gamma_{\text{BCS}}^A + \Gamma_{\text{BCS}}^R$ (2nd and 3rd diagram in Fig. 1(a)) contains only the retarded (advanced) photon GF $D_{R(A)}$, while the fluctuation term Γ_{fluct} (4th diagram in Fig. 1(a)) contains only D_K . Hence, the BCS term Γ_{BCS} is directly affected only by the dispersion and lifetime of the photons, but not by their distribution. On the other hand, the fluctuation term Γ_{fluct} knows about how photon modes are occupied. Correspondingly, while the BCS vertex contains the electron G^K proportional to the Fermi-Dirac distribution, the fluctuation term only contains retarded electron GFs i.e. depends only on the electron dispersion and lifetime but not directly on their distribution.

Since the number of photons is not conserved and in the low-Kelvin regime there is essentially no thermal occupation of an optical cavity on average, the photons can be present only due to vacuum fluctuations (or if we include cavity loss by the corresponding noise, as we shall see later), which explains the nomenclature Γ_{fluct} .

Energy structure of the pairing. Besides their complementarity in terms of the causal structure illustrated above, the fluctuation-induced pairing and the BCS pairing differ sharply in their energy structure. This can be understood by using the separation of energy scales between the on-shell and off-shell electrons, shown in Fig. 1(b). On-shell electrons have frequencies $\omega_1 \sim \epsilon_{k_F \pm q_0}$ (see eq. (3)), where $\epsilon_{k_F \pm q_0}$ is a small characteristic scale i.e. $\epsilon_{k_F \pm q_0} \ll E_F$ as well as $\epsilon_{k_F \pm q_0} \ll \delta_c$. These low energy electrons, highlighted by the blue shell in

Fig. 1(b), are the ones that eventually form the Cooper pairs, as signaled by a divergent pairing amplitude $\Gamma_{\text{on-shell}}$ as a solution to the BS equation (2) for $T < T_c$. On the other hand, off-shell electrons (highlighted by the green shell in Fig. 1(b)) have frequencies close to the photon resonance frequency i.e. far away from the FS: $\omega_1 \sim \delta_c$. Off-shell electrons are not the ones actually building the pair, but can play a crucial role in intermediate scattering processes, as we shall see in the case when the fluctuation term is included.

BCS pairing. As illustrated in Fig. 1(c), here an adiabatic off-shell photon with frequency $\omega_1 - \omega \sim \epsilon_{k_F \pm q_0} \ll \delta_c$, scatters an on-shell electron (corresponding to the peak in G^K around $\omega_1 \sim \epsilon_{k_F \pm q_0}$) to a state which is still in the vicinity of the FS. This state is on-shell since the transferred momentum $q_0 \ll k_F$. In eq. (3), $V^{(0)}D_{R(A)}$ in Γ_{BCS} can thus be substituted by a negative constant $\sim -g_0^2/2\delta_c$ quantifying the net attractive interaction, as in the standard BCS scenario involving phonons. This gives the following equation for T_c^{BCS} (see Appendix C for a detailed derivation [24])

$$4\tilde{g}\delta_c \frac{\tanh\left(\frac{\epsilon_{k_F+q_0}}{2T_c^{\text{BCS}}}\right)}{\epsilon_{k_F+q_0}} = 1. \quad (5)$$

Here, $\tilde{g} = g_0^2/(4\pi\delta_c)^2$ is the dimensionless coupling. We observe that, differently from the standard phonon case, there are no integrals over loop momentum left due to the long-range nature of the photon-mediated interaction: $V^{(0)}(\vec{q}) \propto \delta_{\vec{q}, \pm q_0 \hat{x}}$. For $T \gg \epsilon_{k_F+q_0}$, the linear vanishing $\tanh(x) \simeq x$ of the electron occupation is crucial in cutting off the $1/\epsilon$ divergence at the FS ($\epsilon_{k_F+q_0} \propto q_0$ is finite for finite q_0 but is the smallest scale), yielding $T_c^{\text{BCS}} \sim 2\tilde{g}\delta_c$.

Fluctuation-enhanced pairing. On the other hand, photon fluctuations are concentrated around the cavity resonance frequency, which in the frame of the driving laser corresponds to δ_c . Hence, in the fluctuation term, pairing is mediated by on-shell non-adiabatic photons, with $\omega_1 - \omega \sim \delta_c$ which scatter electrons off shell. The frequency dependence of the photon GF $D^K(\omega) \sim \delta(\omega - \delta_c)$ can never be neglected in eq. (3). Due to the presence of Γ_{fluct} , the BS equation (2) is not diagonal in frequency, as it couples the electronic on-shell and off-shell sectors. As shown in Fig. 1(d), a further scattering process where a second non-adiabatic photon brings the electron back on-shell closes the BS equation. The latter leads to the following equation for the critical temperature (see Appendix D for a detailed derivation [24])

$$\frac{4\tilde{g}\delta_c}{\epsilon_{k_F+q_0}} \tanh\left(\frac{\epsilon_{k_F+q_0}}{2T_c^{\text{fluct}}}\right) + \frac{32}{3} \frac{\tilde{g}^2\delta_c^2}{\epsilon_{k_F+q_0}^2} \left(\coth\frac{\delta_c}{2T_c^{\text{fluct}}}\right)^2 = 1. \quad (6)$$

Note that the BCS contribution (first term on the L.H.S of eq. (6)) depends on the electron occupation, while the non-BCS-type contribution (second term on the L.H.S of eq. (6)) depends on the photon occupation. Fig. 2 (a) shows that the fluctuation-induced pairing significantly enhances superconductivity, leading to a critical temperature T_c^{fluct} (dotted

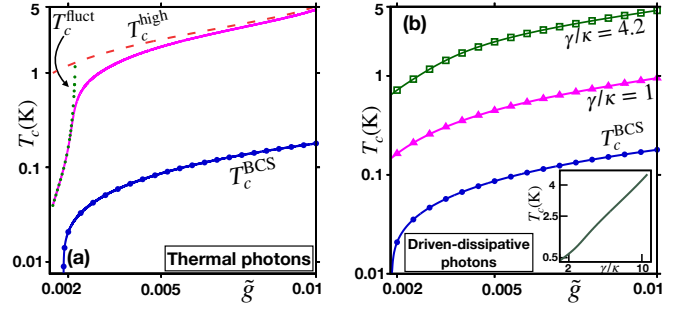


FIG. 2. Critical temperature T_c vs dimensionless coupling strength \tilde{g} in log plot. (a) For thermal photons, the blue solid line with circles corresponds to the prediction 5, based on solely the BCS pairing (see Fig. 1(c)). The magenta solid line corresponds to the prediction which also includes the fluctuation-induced pairing (see Fig. 1(d)), as well as a finite Fermi-liquid-type electron lifetime (see eq. (7)). The green dotted line shows the prediction for long-lived electrons from eq. 6, while the red-dashed line corresponds to the prediction of eq. 8 for short-lived electrons. (b) For driven dissipative photons, solid line with circles shows the BCS prediction which is almost unaffected by photon loss and incoherent pump. Solid lines with triangles show the fluctuation-assisted enhancement in the purely lossy case $\gamma = \kappa$ which is further amplified by incoherent pumping $\gamma > \kappa$ shown by solid line with squares. Inset (linear plot) shows T_c increases almost linearly with γ . We choose $\delta_c = 0.19\text{THz}$, $\epsilon_{k_F+q_0}/\delta_c = 0.007$, $\kappa/\delta_c = 0.01$ and for the inset $\tilde{g} = 0.004$.

green line) increased by an order of magnitude with respect to the BCS prediction T_c^{BCS} (solid line with circles). This enhancement can be understood in the following way: for not too small laser detunings, the average thermal occupation of cavity photons is negligible: $\coth(\delta_c/2T) \sim 1$, so that only vacuum fluctuations remain (later we will discuss the impact of cavity loss and incoherent pump). This allows to obtain the simple expression for the critical temperature $T_c^{\text{fluct}} \sim 2\tilde{g}\delta_c/[1 - 32(\tilde{g}\delta_c)^2/(3\epsilon_{k_F+q_0}^2)]$. For realistic parameters of 2D materials (LAO/STO) coupled to a split-ring cavity [9, 27, 28], the ratio $\delta_c/\epsilon_{k_F+q_0} \sim 135$, and hence the fluctuation-induced term significantly reduces the denominator from 1 already at moderate coupling strengths $\tilde{g} \sim 0.002$, leading to a significant increase in T_c . We also note that the quantities appearing in the 2nd term of eq. (6) are squared due to the additional intermediate scattering to off-shell states described above. The perturbative expansion in terms of such scattering processes is controlled as long as $\tilde{g}, \epsilon_{k_F+q_0}/\delta_c \ll 1$ (see Appendix D [24]). Moreover, for the high-energy and low-momentum photons involved in the non-BCS pairing, in Ref. [29] we show at the non-perturbative level that: a) particle-hole excitations only weakly affect the cavity-photon dynamics as well as the electron pairing; b) higher-order corrections to the electron-photon vertex are small. All these effects are thus safely neglected in our BS equation.

At the current level of description, the finite temperature cannot remove the $1/\epsilon^2$ divergence at the FS arising from the non-BCS-type pairing. In order to remove this divergence, we need to take into account the finite lifetime of electrons.

We consider here a Fermi-liquid scaling of the quasiparticle lifetime in two dimensions [30–32],

$$\frac{1}{\tau_{e,\text{cou}}(T; \epsilon_k)} = \frac{\pi \max(T, \epsilon_k)^2}{8 E_F} \log \left[\frac{E_F}{\max(T, \epsilon_k)} \right], \quad (7)$$

induced by the screened Coulomb interaction between on-shell electrons. This Fermi-liquid lifetime introduces also the leading temperature dependence of the fluctuation-induced pairing. This yields the critical temperature indicated by the solid (magenta) line in Fig. 2(a). For a finite cavity wave vector q_0 and at sufficiently low T , the quasiparticle energy $\epsilon_{k_F+q_0}$ dominates over the broadening $\tau_{e,\text{cou}}^{-1}(T; \epsilon_k)$, so that T_c closely follows the prediction T_c^{fluct} for infinitely-long-lived electrons. T_c is raised further by increasing the coupling \tilde{g} , until the temperature becomes large enough for quasiparticle broadening to become appreciable, leading to the flattening of the critical-temperature curve as a function of \tilde{g} . A large enhancement induced by photon fluctuations still remains compared to BCS prediction. In this regime, $\tau_{e,\text{cou}}^{-1}(T; \epsilon_k) \gg \epsilon_{k_F+q_0}$ and the critical temperature is approximately determined by the following equation (see Appendix E for a detailed derivation [24]):

$$\frac{2\tilde{g}\delta_c}{T_c^{\text{high}}} + \frac{32\tilde{g}^2\delta_c^2}{\tau_{e,\text{cou}}^{-2}(T_c^{\text{high}})} \left(\coth \frac{\delta_c}{2T_c^{\text{high}}} \right)^2 = 1. \quad (8)$$

In the high T limit, T_c^{high} (dashed red line) shows good agreement with the full numerical answer. At this point, it is worthwhile to mention that T_c^{high} is also valid in the limit of vanishing cavity wave vector $q_0 \rightarrow 0$. Referring to the discussion made in the model section, we see that the fluctuation-assisted enhancement of superconductivity thus applies to both the split-ring-cavity geometry considered in Ref.[9] and to the planar microcavity geometry considered in Ref.[7].

Let us show more explicitly that the non-BCS-type pairing induced by fluctuations is appreciable only if the interactions are long ranged i.e. when the bosonic mediator can transfer momenta which are concentrated in a narrow window. In order to obtain a simple estimate, we substitute the delta-function in $V^{(0)}(\vec{q})$ with a box of fixed width. In this case, the factor $1/\tau_{e,\text{cou}}^{-2}$ in the fluctuation term of eq. (8) is replaced by

$$-\frac{1}{2W} \int_{-W}^W \frac{d\epsilon}{\left(\epsilon - \frac{i}{\tau_{e,\text{cou}}}\right) \left(\epsilon - \frac{i}{\tau_{e,\text{cou}}}\right)} = \frac{1}{W^2 + \tau_{e,\text{cou}}^{-2}}, \quad (9)$$

where W is the box-width in units of energy. If the width W exceeds the inverse electron lifetime $\tau_{e,\text{cou}}^{-1}$ at the Fermi surface, the fluctuation-induced enhancement of pairing ($\propto \delta_c^2/W^2$) will be cut off. This explains why the effect discussed in this work is not relevant for the standard phonon-mediated pairing. There the energy window W is set by the Debye frequency, which is large compared to electronic scales. In this regime, the BCS term takes the known logarithmic form

$$T_c^{\text{BCS}} \propto W \exp(-W/(\tilde{g}\delta_c)).$$

Impact of photon loss and incoherent pump. Photon loss out of the cavity mirrors is unavoidable and typically happens at an appreciable rate γ_{loss} . The resulting damping of photons is introduced in the retarded/advanced GFs $D_{R/A}$ in Eq. 4 by substituting $0^+ \rightarrow \kappa$, while the corresponding noise is included through the Keldysh GF [33–35] as

$$D_K(\vec{q}, \omega) = -i \frac{\gamma}{\delta_c} \frac{\omega^2 + \kappa^2 + \delta_c^2}{(\omega^2 - \kappa^2 - \delta_c^2)^2 + 4\kappa^2\omega^2}. \quad (10)$$

Here the parameter γ quantifies the noise level. If, apart from the coherent laser drive, the cavity is not further illuminated, then $\gamma = \kappa = \gamma_{\text{loss}}/2$ i.e. the loss rate sets both the damping and the noise. We will also study the effect of an incoherent pump (as resulting from a broadband illumination) at rate $\gamma_{\text{pump}} < \gamma_{\text{loss}}$. In this case the net loss rate becomes $\kappa = (\gamma_{\text{loss}} - \gamma_{\text{pump}})/2$ while the total noise level $\gamma = (\gamma_{\text{loss}} + \gamma_{\text{pump}})/2 > \kappa$. For any finite cavity-loss rate, inelastic electron-photon scattering further reduces the electron lifetime: $\tau_e^{-1} = \tau_{e,\text{cou}}^{-1} + \tau_{e,\text{cav}}^{-1}$, with $\tau_{e,\text{cav}}^{-1} \simeq 2\tilde{g}\gamma/(1 + \kappa^2/\delta_c^2)$ (see Appendix F [24]). Assuming $\delta_c \gg \kappa$ and $\tau_e^{-1} \gg \epsilon_{k_F+q_0}$, the equation for the critical temperature takes the simple form (see Appendix F [24] for a detailed derivation):

$$\frac{2\tilde{g}\delta_c}{T_c^{\text{noise}}} + 4\tilde{g}^2 \frac{\gamma^2}{\kappa^2} \frac{\delta_c^2}{\tau_e^{-2}(T_c^{\text{noise}})} \left[1 - \frac{1}{1 + \frac{\tau_e^{-1}(T_c^{\text{noise}})}{2\kappa}} \right] = 1. \quad (11)$$

This time we used T_c^{noise} as opposed to T_c^{fluct} , since the presence of a on-shell photon is not due to vacuum fluctuations but to loss-induced noise or, at finite pump rates, to a finite average occupation of the cavity mode. We see indeed that the thermal \coth is replaced here by $\gamma/\kappa = 1 + 2n_{\text{ph}}$, with n_{ph} being the average incoherent occupation of the cavity. When γ_{pump} approaches γ_{loss} our model needs to be extended to include pump saturation that prevents the divergence in the photon number. T_c^{noise} is shown in Fig. 2(b). While the BCS prediction $T_c^{\text{BCS}} \simeq 2\tilde{g}\delta_c/(1 + \kappa^2/\delta_c^2)$ (Fig. 2(b) with circles) remains essentially unaffected by loss (for $\delta_c \gg \kappa$) and does not depend on incoherent pumping, the non-BCS-type pairing still provides a strong enhancement of superconductivity (Fig. 2(b) with triangles), which is further amplified by a finite incoherent-pump rate (Fig. 2(b) with squares). By comparing eq. (11) with the closed-system expression, we see that for $\kappa \neq 0$ the critical temperature is reduced by the second term in the square bracket. Still, for $\kappa\tau_e \ll 1$ the reduction is negligible. Moreover, by increasing the incoherent-pump rate γ we can further increase T_c almost linearly, as shown in the inset of Fig. 2(b). Hence, with increasing γ , $\tau_{e,\text{cou}}^{-1}$ increases faster ($\propto T^2 \log T$) than the linearly increasing $\tau_{e,\text{cav}}^{-1}$. The Coulomb lifetime thus still serves as the dominant quasiparticle-damping process. For this reason, the photon-induced redistribution of quasiparticles, predicted to be appreciable in certain cavity setups [4] and observed by proper irradiation [36, 37], can instead be neglected in our case. We can predict an increase in T_c as long as the Fermi-

liquid behavior (7) still holds, which sets T_c in the range of the Fermi temperature T_F ($\sim 13\text{K}$ for the materials considered in Ref. [9]).

Conclusions. We have shown that cavity-mediated interactions between electrons induce a non-BCS-type of pairing mechanism triggered by non-adiabatic photon fluctuations, which can largely enhance the superconducting critical temperature T_c under realistic conditions. The characteristic non-BCS dependence of T_c on the tuneable light-matter coupling could be experimentally observed. Moreover, an increase of T_c with the number incoherent photons in the cavity would be indicative of the present non-BCS pairing to be active. These features could be also theoretically reproduced using quantum Monte Carlo for fermion-boson systems[38], proper extensions to long-range interactions of matrix product states[39] or density functional theory [40], as well as finite-frequency extensions of functional renormalization group technique [41].

We thank Bernhard Frank, Dieter Jaksch, Johannes Lang, Andrew Millis, Frank Schlawin, and Michael Sentef for useful discussions.

-
- [1] G. L. Paravicini-Bagliani, F. Appugliese, E. Richter, F. Valmorra, J. Keller, M. Beck, N. Bartolo, C. Rössler, T. Ihn, K. Ensslin, C. Ciuti, G. Scalari, and J. Faist, *Nature Physics* **15**, 186 (2019).
- [2] A. Thomas, E. Devaux, K. Nagarajan, T. Chervy, M. Seidel, D. Hagenmüller, S. Schütz, J. Schachenmayer, C. Genet, G. Pupillo, and T. W. Ebbesen, (2019), [arXiv:1911.01459](https://arxiv.org/abs/1911.01459).
- [3] M. A. Sentef, M. Ruggenthaler, and A. Rubio, *Science Advances* **4**, eaau6969 (2018).
- [4] J. B. Curtis, Z. M. Raines, A. A. Allocca, M. Hafezi, and V. M. Galitski, *Physical Review Letters* **122**, 167002 (2019).
- [5] G. Mazza and A. Georges, *Physical Review Letters* **122**, 17401 (2019).
- [6] M. Kiffner, J. R. Coulthard, F. Schlawin, A. Ardavan, and D. Jaksch, *Physical Review B* **99**, 085116 (2019).
- [7] F. Schlawin, A. Cavalleri, and D. Jaksch, *Physical Review Letters* **122**, 133602 (2019).
- [8] A. A. Allocca, Z. M. Raines, J. B. Curtis, and V. M. Galitski, *Phys. Rev. B* **99**, 020504 (2019).
- [9] H. Gao, F. Schlawin, M. Buzzi, A. Cavalleri, and D. Jaksch, *Phys. Rev. Lett.* **125**, 053602 (2020).
- [10] Y. Ashida, A. Imamoglu, J. Faist, D. Jaksch, A. Cavalleri, and E. Demler, (2020), [arXiv:2003.13695](https://arxiv.org/abs/2003.13695).
- [11] M. A. Sentef, J. Li, F. Künzel, and M. Eckstein, *Physical Review Research* **2**, 033033 (2020).
- [12] F. Piazza and P. Strack, *Physical Review Letters* **112**, 143003 (2014).
- [13] J. Keeling, M. J. Bhaseen, and B. D. Simons, *Physical Review Letters* **112**, 143002 (2014).
- [14] Y. Chen, Z. Yu, and H. Zhai, *Physical Review Letters* **112**, 143004 (2014).
- [15] F. Piazza and P. Strack, *Physical Review A* **90**, 043823 (2014).
- [16] J.-S. Pan, X.-J. Liu, W. Zhang, W. Yi, and G.-C. Guo, *Physical Review Letters* **115**, 045303 (2015).
- [17] W. Zheng and N. R. Cooper, *Physical Review Letters* **117**, 175302 (2016), [arXiv:1604.06630](https://arxiv.org/abs/1604.06630).
- [18] C. Kollath, A. Sheikhan, S. Wolff, and F. Brennecke, *Physical Review Letters* **116**, 060401 (2016), [arXiv:1502.01817](https://arxiv.org/abs/1502.01817).
- [19] F. Mivehvar, H. Ritsch, and F. Piazza, *Physical Review Letters* **118**, 073602 (2017).
- [20] E. Colella, R. Citro, M. Barsanti, D. Rossini, and M.-L. Chiofalo, *Physical Review B* **97**, 134502 (2018).
- [21] F. Mivehvar, H. Ritsch, and F. Piazza, *Physical Review Letters* **122**, 113603 (2019).
- [22] F. Schlawin and D. Jaksch, *Physical Review Letters* **123**, 133601 (2019).
- [23] A. A. Abrikosov, I. Dzyaloshinskii, L. P. Gorkov, and R. A. Silverman, *Methods of quantum field theory in statistical physics* (Dover, New York, NY, 1975).
- [24] See Supplemental Material for the derivation of the effective action using the Schwinger-Keldysh field theoretic technique, the solution of the resultant Bethe-Salpeter equation for the vertex-function to find critical temperature including both the standard BCS and the new non-BCS mechanisms, a discussion on the effect of finite life-time of the electrons and the role cavity-losses and incoherent pumping, which includes Refs. [42–44].
- [25] R. D. Mattuck, *Methods of Quantum Field Theory in Statistical Physics* (Dover Publications, INC. New York, 1992).
- [26] A. Kamenev, *Field theory of non-equilibrium systems* (Cambridge University Press, 2011).
- [27] T. Sakudo and H. Unoki, *Phys. Rev. Lett.* **26**, 851 (1971).
- [28] X. Lin, Z. Zhu, B. Fauqué, and K. Behnia, *Phys. Rev. X* **3**, 021002 (2013).
- [29] A. Chakraborty and F. Piazza, to appear.
- [30] G. F. Giuliani and J. J. Quinn, *Physical Review B* **26**, 4421 (1982).
- [31] L. Zheng and S. Das Sarma, *Phys. Rev. B* **53**, 9964 (1996).
- [32] T. Jungwirth and A. H. MacDonald, *Phys. Rev. B* **53**, 7403 (1996).
- [33] E. G. D. Torre, S. Diehl, M. D. Lukin, S. Sachdev, and P. Strack, *Phys. Rev. A* **87**, 023831 (2013).
- [34] L. M. Sieberer, M. Buchhold, and S. Diehl, *Reports on Progress in Physics* **79**, 096001 (2016).
- [35] J. Lang, D. E. Chang, and F. Piazza, “Non-equilibrium diagrammatic approach to strongly interacting photons,” (2018), [arXiv:1810.12921 \[cond-mat.quant-gas\]](https://arxiv.org/abs/1810.12921).
- [36] T. Klapwijk and P. de Visser, *Annals of Physics* **417**, 168104 (2020).
- [37] K. S. Tikhonov, A. V. Semenov, I. A. Devyatov, and M. A. Skvortsov, *Annals of Physics* **417**, 168101 (2020).
- [38] S. Beyl, F. Goth, and F. F. Assaad, *Phys. Rev. B* **97**, 085144 (2018).
- [39] C.-M. Halati, A. Sheikhan, and C. Kollath, *Phys. Rev. Research* **2**, 043255 (2020).
- [40] P. de Silva, T. Zhu, and T. Van Voorhis, *The Journal of Chemical Physics* **146**, 024111 (2017), <https://doi.org/10.1063/1.4973728>.
- [41] C. Karrasch, R. Hedden, R. Peters, T. Pruschke, K. Schönhammer, and V. Meden, *Journal of Physics: Condensed Matter* **20**, 345205 (2008).
- [42] J. W. Negele and H. Orland, *Quantum Many Body Systems* (Oxford University Press on Demand, 2002).
- [43] A. Altland and B. D. Simons, *Condensed matter field theory* (Cambridge University Press, 2010).
- [44] D. Pines and P. Nozières, *The theory of quantum liquids normal fermi liquids* (2018) pp. 1–180.

Supplementary Material for “Long-Range Photon Fluctuations Enhance Photon-Mediated Electron Pairing and Superconductivity”

Ahana Chakraborty^{1,*} and Francesco Piazza^{1,†}

¹Max Planck Institute for the Physics of Complex Systems, Nöthnitzer Str. 38, 01187, Dresden, Germany.

(Dated: November 15, 2021)

Appendix A: Effective Electron-Electron Interaction Mediated by Photons

In the main text, we analyze the pairing instability leading to superconducting transition in the coupled light-matter system. We consider a 2D electron system described by the Hamiltonian,

$$H_e = \sum_{\vec{k}, \sigma} \epsilon_k c_{\vec{k}, \sigma}^\dagger c_{\vec{k}, \sigma}, \quad (\text{A1})$$

where $c_{\vec{k}, \sigma}^\dagger$ is the creation operator of an electron of momentum, \vec{k} and spin σ . The dispersion of the non-interacting electrons with effective mass, m^* is given by $\epsilon_k = |\vec{k}|^2/2m^* - E_F$, where the electronic energy is measured from the Fermi surface, at $\vec{k} = \vec{k}_F$. The 2D electron system is coupled to a tera-Hertz optical cavity which supports a single mode of frequency ω_c and momentum $q_0 \hat{x}$ with $q_0 = \omega_c \sqrt{\epsilon_r}/c$. The coupled light-matter system is placed under a vertical beam of laser of frequency ω_L , which is detuned from the cavity frequency by $\delta_c = \omega_c - \omega_L$. We consider the detuning to be large enough so that the optical cavity is perfectly transparent at the frequency of the laser. In the frame rotating with the Laser frequency ω_L , the cavity Hamiltonian takes the form,

$$H_c = \delta_c b^\dagger b, \quad (\text{A2})$$

where b^\dagger is the creation operator of cavity photons of momentum \vec{q}_0 . The electron Hamiltonian is unaffected by the rotation of the reference frame. In presence of strong driving by the external Laser beam, the dominant light-matter interaction is induced via the two-photon diamagnetic process which leads to coupling between the electrons and photons in the density channel given by¹,

$$H_{\text{light-matter}} = \sum_{\vec{k}, \sigma} \sum_{\vec{q} = \pm q_0 \hat{x}} g_0 c_{\vec{k} + \vec{q}, \sigma}^\dagger c_{\vec{k}, \sigma} (b + b^\dagger). \quad (\text{A3})$$

Here, the strength of the light-matter coupling, $g_0 \propto \sqrt{I_d} \omega_c / \omega_L$ which is directly tunable by the intensity I_d of the external laser beam¹. For the numerical calculations shown in the main text, we use the set of parameters for the electronic system consistent with 2D interface between lanthanum titanate (LAO) and strontium titanate (STO) in normal phase and for photons consistent with a split-ring cavity, given by¹⁻³,

$$E_F = 0.266 \text{ THz}, \quad m^* = 2m_e, \quad \epsilon_{k_F + q_0} = 1.4 \times 10^{-3} \text{ THz}, \quad \omega_c = 2\pi \times 0.3 \text{ THz}, \quad \delta_c = 0.1\omega_c, \quad \epsilon_r = 10^4. \quad (\text{A4})$$

We use the real time formulation of non-equilibrium field theory⁴ to analyze the superconducting transition in the coupled light-matter system. Schwinger-Keldysh (SK) field theory formalism provides an efficient tool to study driven-dissipative systems as well as systems in equilibrium. In the latter case, SK field theory is completely an equivalent formulation of the standard Matsubara field theory⁵. In this appendix, we will derive the effective action describing the electron-electron interaction mediated by the cavity photons.

In SK field theory formalism, the evolution of a many body density matrix, $\hat{\rho}(t) = U(t, 0) \hat{\rho}_0 U^\dagger(t, 0)$, is represented by two path integrals involving two copies of fields, $\phi_+(r, t)$ and $\phi_-(r, t)$, where r denotes any single particle index. These fields correspond to the forward and backward evolution of real time t , represented by $U(t, 0)$ and $U^\dagger(t, 0)$ respectively. These two path integrals are not independent, rather connected by the initial density matrix, $\hat{\rho}_0$ at $t = 0$. Hence, to get rid of the redundancy, it is convenient to work in a rotated basis, $\phi_{cl, q} = (\phi_+ \pm \phi_-)/\sqrt{2}$. In the (cl, q) basis, we define two independent Green's functions of SK field theory, namely retarded (advanced) Green's functions, $G_{R(A)}(r, t; r', t')$ and the Keldysh Green's function, $G_K(r, t; r', t')$, given by,

$$G_R(r, t; r', t') = \langle \phi_{cl}(r, t) \phi_q^*(r', t') \rangle, \quad G_K(r, t; r', t') = \langle \phi_{cl}(r, t) \phi_{cl}^*(r', t') \rangle. \quad (\text{A5})$$

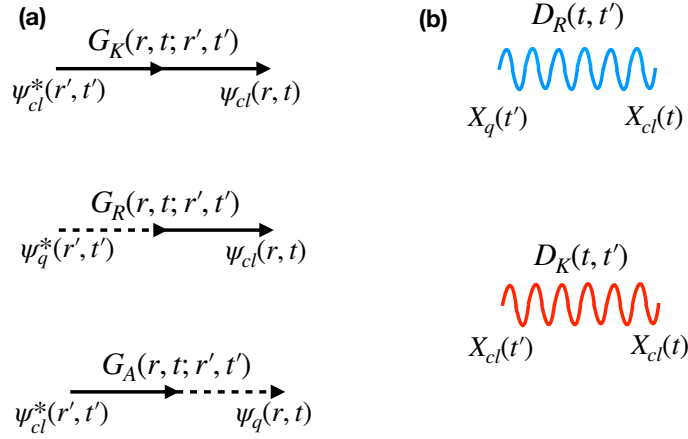


Figure 1. (a) Green's functions for Fermions, involving the Grassmann fields, $\psi_{cl,q} = (\psi_+ \pm \psi_-)/\sqrt{2}$. G_R (G_A) is the retarded (advanced) component and G_K is the Keldysh component. Here the classical and the quantum fields are denoted by the solid and dashed lines respectively. (b) Green's functions for the cavity photons, involving the real Bosonic fields, $X_{cl,q} = (X_+ \pm X_-)/2$. The retarded component, D_R is represented by the blue curvy line while the Keldysh component, D_K is represented by the red curvy line.

The causal structure of the Green's functions is ensured by $G_A = G_R^\dagger$ and $G_K = -G_K^\dagger$. $G_{R(A)}$ only contains information about spectrum and lifetime of the system, while G_K explicitly depends on the distribution function of the system. In thermal equilibrium, these two Green's functions are related by the Fluctuation-Dissipation theorem (FDT)⁴,

$$G_K(r, r'; \omega) = 2 \text{Im} [G_R(r, r'; \omega)] F(\omega), \quad (\text{A6})$$

where, $F(\omega) = [\tanh(\omega/2T)]^{-\zeta}$ is the thermal distribution function of the system, with $\zeta = \pm 1$ for Bosons and Fermions respectively.

In the case of our particular interest in this work, the Green's functions, $G_{R(A)}$ and G_K for the 2D electrons involving the Grassmann fields $\psi_{cl(q)}(r, t)$ (coherent states of the Fermionic creation-annihilation operator) are shown in Fig. 1(a). Here the solid and dashed lines represent the the classical and quantum Grassmann fields respectively. In this case, the Schwinger-Keldysh action for the 2D electrons described by the Hamiltonian in Eq.A1 is diagonal in the frequency-momentum basis and take the form,

$$S_e = \int_{-\infty}^{\infty} \frac{d\omega}{2\pi} \sum_{\vec{k}, \sigma} \Psi^\dagger(\vec{k}, \omega) \begin{bmatrix} 0 & G_A^{-1} \\ G_R^{-1} & [G_K]^{-1} \end{bmatrix} \Psi(\vec{k}, \omega), \quad (\text{A7})$$

where, $\Psi^\dagger = [\psi_{cl, \sigma}^*, \psi_{q, \sigma}^*]$. Here, $G_{R(A)}^{-1}$ and $[G_K]^{-1}$ are the retarded (advanced) and the Keldysh component of the inverse Green's functions of electrons. For non-interacting electrons in thermal equilibrium, the bare inverse Green's functions are given by, $G_{R(A)}^{-1} = w - \epsilon_k \pm i0^+$ and $[G_K]^{-1}$ is a purely imaginary regulatory term. Inverting the kernel in Eq. A7, we obtain the thermal Green's functions of the non-interacting electrons at temperature T of the form,

$$G_{R(A)}(\vec{k}, \omega) = \frac{1}{w - \epsilon_k \pm i0^+}, \quad G_K(\vec{k}, \omega) = -2\pi i \tanh\left(\frac{\omega}{2T}\right) \delta(\omega - \epsilon_k). \quad (\text{A8})$$

In sections C and D, we use these bare Green's functions of the thermal electrons to calculate the pairing instability of the system. These bare Green's functions will be further dressed by the self-energies induced by the screened Coulomb repulsion between the 2D electrons. This introduces finite lifetime of the quasi-particles which we will discuss in section E.

Next, we consider the system of photons in the driven optical cavity. Guided by the form of the light-matter interaction Hamiltonian (Eq. A3), where the density operator of the electrons couple to the position operator of the photons $x = (b + b^\dagger)/\sqrt{2\delta_c}$, we represent photons by the real Bosonic fields, $X_\pm(t)$. They are related to the complex Bosonic fields, $\chi_\pm(t)$ (coherent states of the creation-annihilation operators of photons) by⁴,

$$X_\pm(t) = \frac{1}{\sqrt{2\delta_c}} [\chi_\pm(t) + \chi_\pm^*(t)]. \quad (\text{A9})$$

The Green's functions of the photons in terms of the real scalar fields, $X_{cl(q)} = [X_+ \pm X_-]/2$ are shown in Fig.1(b). Here, the

blue and red curvy lines represent the retarded (D_R) and Keldysh (D_K) Green's functions of the photons respectively. For real Bosonic fields, $D_R(t, t') = D_A(t', t)$. In this basis, the SK action for the single mode cavity in the rotating frame takes the form,

$$S_c = \int_{-\infty}^{\infty} \frac{d\omega}{2\pi} \hat{X}^T(\omega) \begin{bmatrix} 0 & D_A^{-1} \\ D_R^{-1} & [D_K]^{-1} \end{bmatrix} \hat{X}(\omega), \quad (\text{A10})$$

where $\hat{X}^T = [X_{cl}, X_q]$. Here, $D_{R(A)}^{-1}$ and $[D_K]^{-1}$ are the retarded (advanced) and the Keldysh component of the inverse Green's functions of photons. In case of the cavity photons in thermal equilibrium at temperature T , the bare inverse Green's functions take the form, $D_{R(A)}^{-1} = (\omega \pm i0^+)^2 - \delta_c^2$ and $[D_K]^{-1}$ is a purely imaginary regulatory term. Inverting the kernel in Eq. A10, we obtain the thermal Green's functions of the bare photons at temperature T of the form,

$$D_{R(A)}(\omega) = \frac{1}{2} \frac{1}{(\omega \pm i0^+)^2 - \delta_c^2}, \quad D_K(\omega) = \frac{1}{2} \frac{(-\pi i)}{\delta_c} [\delta(\omega - \delta_c) - \delta(\omega + \delta_c)] \coth\left(\frac{\omega}{2T}\right). \quad (\text{A11})$$

We note that in case of a single mode, the dispersion of the cavity photons is replaced by the shifted energy of the mode, δ_c in the rotating frame. In the subsequent appendices C, D, E, we will restrict our discussion to the case of thermal photons in equilibrium with the 2D electrons at temperature, T . We postpone the discussion on the case of driven-dissipative photons to appendix F.

Next, we write the Keldysh action corresponding to the light-matter interaction Hamiltonian (Eq. A3) of the form,

$$S_{\text{light-matter}} = -g_0 \sqrt{2\delta_c} \int_{-\infty}^{\infty} dt \sum_{\vec{k}, \sigma} \sum_{\vec{q}=\pm q_0 \hat{x}} \left[\{\psi_{cl, \sigma}^*(\vec{k} + \vec{q}, t) \psi_{q, \sigma}(\vec{k}, t) + cl \leftrightarrow q\} X_{cl}(t) \right. \\ \left. + \{\psi_{cl, \sigma}^*(\vec{k} + \vec{q}, t) \psi_{cl, \sigma}(\vec{k}, t) + cl \leftrightarrow q\} X_q(t) \right] \quad (\text{A12})$$

After integrating out the quadratic action of the photons, we generate the cavity-mediated effective electron-electron interaction of the form,

$$S_{eff} = - \int \int d\omega d\omega_1 \sum_{\vec{p}, \vec{k}, \sigma, \sigma'} V^{(0)}(\vec{k} - \vec{p}) \\ \left[D_R(\omega_1 - \omega) \left[\psi_{cl, \sigma}^*(\vec{k}, \omega_1) \{ \psi_{cl, \sigma'}^*(-\vec{k}, -\omega_1) \psi_{cl, \sigma'}(-\vec{p}, -\omega) + cl \leftrightarrow q \} \psi_{q, \sigma}(\vec{p}, \omega) \right. \right. \\ \left. \left. + \psi_{q, \sigma}^*(\vec{k}, \omega_1) \{ \psi_{cl, \sigma'}^*(-\vec{k}, -\omega_1) \psi_{cl, \sigma'}(-\vec{p}, -\omega) + cl \leftrightarrow q \} \psi_{cl, \sigma}(\vec{p}, \omega) \right] \right. \\ \left. + D_A(\omega_1 - \omega) \left[\psi_{cl, \sigma}^*(\vec{k}, \omega_1) \{ \psi_{cl, \sigma'}^*(-\vec{k}, -\omega_1) \psi_{q, \sigma'}(-\vec{p}, -\omega) + cl \leftrightarrow q \} \psi_{cl, \sigma}(\vec{p}, \omega) \right. \right. \\ \left. \left. + \psi_{q, \sigma}^*(\vec{k}, \omega_1) \{ \psi_{cl, \sigma'}^*(-\vec{k}, -\omega_1) \psi_{q, \sigma'}(-\vec{p}, -\omega) + cl \leftrightarrow q \} \psi_{q, \sigma}(\vec{p}, \omega) \right] \right. \\ \left. + D_K(\omega_1 - \omega) \left[\psi_{cl, \sigma}^*(\vec{k}, \omega_1) \{ \psi_{cl, \sigma'}^*(-\vec{k}, -\omega_1) \psi_{q, \sigma'}(-\vec{p}, -\omega) + cl \leftrightarrow q \} \psi_{q, \sigma}(\vec{p}, \omega) \right. \right. \\ \left. \left. + \psi_{q, \sigma}^*(\vec{k}, \omega_1) \{ \psi_{cl, \sigma'}^*(-\vec{k}, -\omega_1) \psi_{q, \sigma'}(-\vec{p}, -\omega) + cl \leftrightarrow q \} \psi_{cl, \sigma}(\vec{p}, \omega) \right] \right]. \quad (\text{A13})$$

Here $V^{(0)}(\vec{q}) = g_0^2 \delta_c \delta_{\vec{q}, \pm q_0 \hat{x}}$ is the coupling function. In the Keldysh space, this electron-electron interaction is represented by 12 bare interaction vertices, as shown in Fig 2. Out of them, 4 interaction vertices are mediated by the retarded propagation of photons, D_R , shown by blue curvy lines in Fig 2 (a). Similar 4 vertices are mediated by advanced propagation of photons, D_A (not shown in the figure). These vertices are responsible to give rise to attractive interaction between electrons, i.e in the adiabatic limit, where the relaxation frequency, $\omega_1 - \omega$, of the mediator bosons is much smaller than their characteristics energy, δ_c , these vertices reduce to,

$$V^{(0)}(\vec{k} - \vec{p}) D_R(\omega_1 - \omega) \simeq g_0^2 \delta_c \frac{(-1)}{2\delta_c^2} \delta_{\vec{k} - \vec{p}, \pm q_0 \hat{x}} = -\frac{g_0^2}{2\delta_c} \delta_{\vec{k} - \vec{p}, \pm q_0 \hat{x}}. \quad (\text{A14})$$

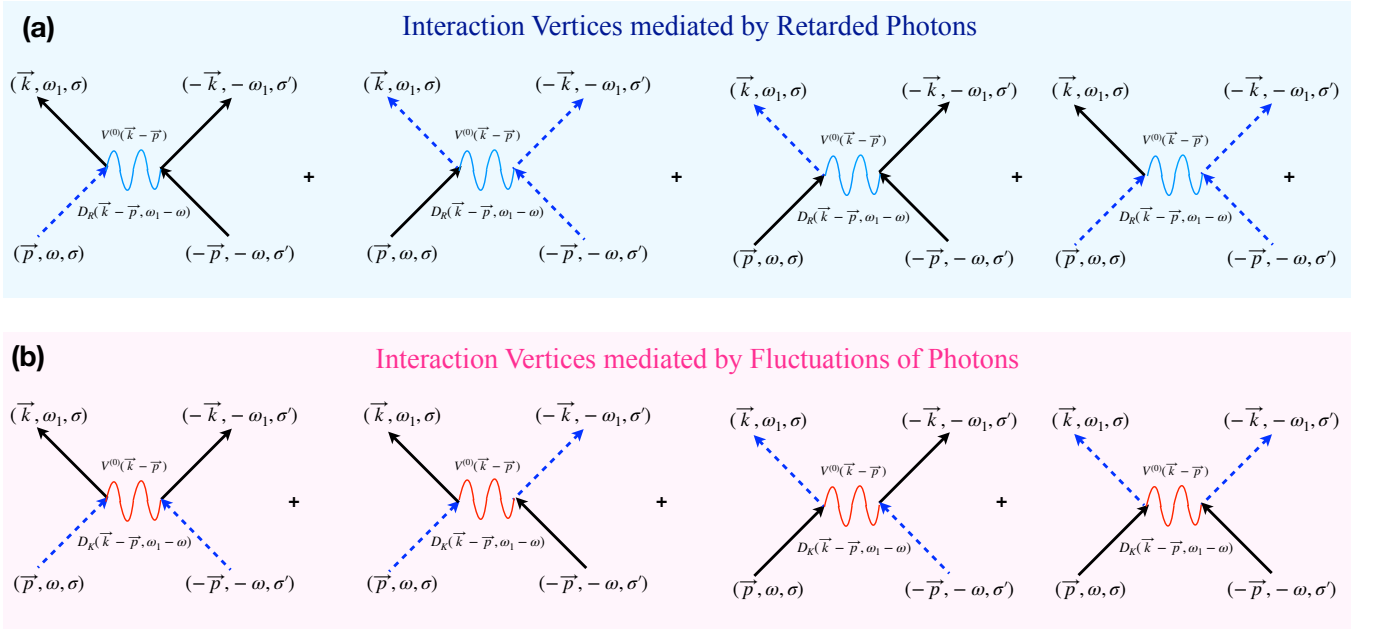


Figure 2. The light-matter coupling Hamiltonian given in Eq. [A3] generates 12 effective electron-electron interaction vertices. Electrons and photons are represented by straight and curvy lines respectively. (a) shows the 4 interaction vertices which are mediated by the Retarded propagator of the cavity photons. Similar 4 vertices mediated by advanced propagator of photons are not shown in the figure. In the adiabatic limit, these standard “BCS” vertices lead to attractive interactions between electrons near Fermi surface and formation of Cooper pair. (b) shows the 4 electron-electron interaction vertices which consist of Keldysh propagator of the mediator photons. These vertices explicitly depend the distribution function of the photons. We propose a new mechanism for pairing low-energy electrons, originating from these “fluctuation” vertices, leading to significant enhancement of the pairing instability in the 2D electron system.

This attractive interaction leads to the pairing instability to form cooper pairs via the standard BCS mechanism^{6,7}.

In addition to these vertices, the light-matter coupling generates 4 more vertices which are mediated by the Keldysh propagator of the cavity photons, represented by red curvy lines in Fig 2(b). These vertices, which are mediated by fluctuations of the photons, further assist the pairing between the low-energy electrons, leading to significant enhancement of the transition temperature, T_c . This is main finding of the work which will be discussed in the next sections.

We note that it has been argued in Ref [1] that at high temperatures, $T > 30mK$, this cavity mediated long ranged interaction between the two dimensional electrons can not be effectively screened by the electron gas. Hence we will restrict ourselves to this un-screened cavity-mediated e-e interaction for the subsequent analysis in this paper.

Appendix B: Pairing Instability in Cooper Channel

In this section, we will investigate the pairing instability in the 2D electron system mediated by the light-matter coupling. To obtain the superconducting transition temperature, we will analyze the divergence the four-point vertex function Γ in the pairing channel coming from repeated scattering of the incoming electrons leading to formation of Cooper pair below the critical temperature. We denote the momenta and frequencies of the incoming electrons by $(\vec{P} + \vec{p}, \Omega + \omega)$ and $(\vec{P} - \vec{p}, \Omega - \omega)$ while those for the outgoing electrons are given by $(\vec{P} + \vec{p}', \Omega + \omega')$ and $(\vec{P} - \vec{p}', \Omega - \omega')$. In general the vertex function $\Gamma(\vec{P}, \Omega; \vec{p}, \omega; \vec{p}', \omega')$ depends on three variables, which are chosen to be the center of mass (COM) coordinates, the relative incoming coordinates and the relative outgoing coordinates. Γ is obtained by solving the Bethe-Salpeter (BS) equation, which is a Dyson-type equation for the four point vertex functions, calculated within the ladder approximation⁸. This equation is in general a complicated coupled equation in relative incoming momenta and frequencies as well as in the Keldysh space between 12 vertices shown in Fig. 2.

We will first analyze the structure of the BS equations in the Keldysh space. The 12 BS equations corresponding to 12 effective four point vertices shown in Fig. 2 have block diagonal structure in Keldysh space. The particular BS equation we will

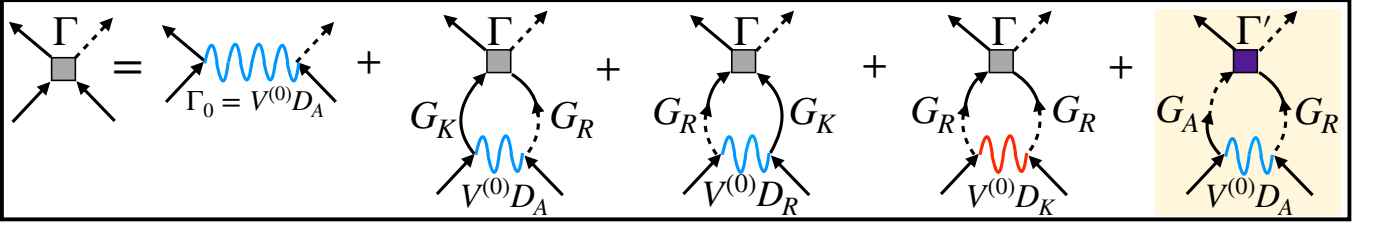


Figure 3. This Bethe-Salpeter equation for the vertex function, Γ , in the pairing channel closes in Keldysh space when of the last (highlighted) term vanishes. This is achieved in the adiabatic limit, when the mediator boson relaxes much slower than its characteristics frequency. The resultant BS equation (without the highlighted term) is a coupled equation only in incoming momenta and frequencies. The first term is the bare vertex, Γ_0 . The second and third terms, Γ_{BCS} , are mediated by advanced and retarded propagators of photons respectively. The fourth term, Γ_{fluct} , includes the effect of photon fluctuations which leads to non-BCS type pairing mechanism described in the main text.

investigate to obtain T_c is shown in Fig. 3 and given by,

$$\begin{aligned}
\Gamma(\vec{P}, \Omega; \vec{p}, \omega; \vec{p}', \omega') &= V^{(0)}(\vec{p}' - \vec{p})D^A(\omega' - \omega) \\
&+ \mathbf{i} \int \frac{d\vec{k}}{(2\pi)^2} \frac{d\omega_1}{2\pi} V^{(0)}(\vec{k} - \vec{p})D_A(\omega_1 - \omega) G_K(\vec{P} + \vec{k}, \Omega + \omega_1) G_R(\vec{P} - \vec{k}, \Omega - \omega_1) \Gamma(\vec{P}, \Omega; \vec{k}, \omega_1; \vec{p}', \omega') \\
&+ \mathbf{i} \int \frac{d\vec{k}}{(2\pi)^2} \frac{d\omega_1}{2\pi} V^{(0)}(\vec{k} - \vec{p})D_R(\omega_1 - \omega) G_R(\vec{P} + \vec{k}, \Omega + \omega_1) G_K(\vec{P} - \vec{k}, \Omega - \omega_1) \Gamma(\vec{P}, \Omega; \vec{k}, \omega_1; \vec{p}', \omega') \\
&+ \mathbf{i} \int \frac{d\vec{k}}{(2\pi)^2} \frac{d\omega_1}{2\pi} V^{(0)}(\vec{k} - \vec{p})D_K(\omega_1 - \omega) G_R(\vec{P} + \vec{k}, \Omega + \omega_1) G_R(\vec{P} - \vec{k}, \Omega - \omega_1) \Gamma(\vec{P}, \Omega; \vec{k}, \omega_1; \vec{p}', \omega') \\
&+ \mathbf{i} \int \frac{d\vec{k}}{(2\pi)^2} \frac{d\omega_1}{2\pi} V^{(0)}(\vec{k} - \vec{p})D_A(\omega_1 - \omega) G_A(\vec{P} + \vec{k}, \Omega + \omega_1) G_R(\vec{P} - \vec{k}, \Omega - \omega_1) \Gamma'(\vec{P}, \Omega; \vec{k}, \omega_1; \vec{p}', \omega'). \quad (\text{B1})
\end{aligned}$$

At the transition temperature, we set the COM frequency $\Omega = 0$ as well as the COM momentum $\vec{P} = 0$, as the Cooper pair is at rest in COM frame⁷. Moreover, the above equation for Γ is completely decoupled in the 1st and 3rd coordinates, i.e in COM coordinates and the relative coordinates of the outgoing electrons. Hence for the sake of simplicity of notation, we will denote Γ only by keeping the relative coordinates of the incoming electrons, i.e $\Gamma(\vec{p}, \omega)$ for the rest of the discussion and also in the main text.

We note that in Eq. B1, the last term in R.H.S (highlighted in Fig. 3) is solely responsible for coupling the equation in Keldysh space between two different vertices Γ and Γ' . By the causality structure of the retarded and advanced Green's functions, we observe that in this term all the Green's functions, $D_A(\omega_1 - \omega)$, $G_A(\vec{k}, \omega_1)$ and $G_R(-\vec{k}, -\omega_1)$ have poles w.r.t ω_1 in the upper half plane in the complex frequency plane of ω_1 . Hence, using the contour integration method we can perform the frequency integral over ω_1 by the choosing the other half plane (i.e. the lower half plane) and the above term vanishes. We note that $\Gamma(\vec{P}, \Omega; \vec{k}, \omega_1; \vec{p}', \omega')$ also has pole as a function of the transferred frequency between the incoming and outgoing electrons, $\omega' - \omega_1$, in the complex plane whose residue only adds to the bare vertex part in the BS equation and will not be relevant for the discussion of finding T_c here. Hence, in absence of the last term (highlighted) shown in Fig. 3, the BS equation closes in the Keldysh space. This equation is still a coupled equation in relative incoming momentum and frequencies having the following form,

$$\Gamma(\vec{p}, \omega) = V^{(0)}(\vec{p}' - \vec{p})D^A(\omega' - \omega) + \Gamma_{BCS}^A(\vec{p}, \omega) + \Gamma_{BCS}^R(\vec{p}, \omega) + \Gamma_{\text{fluct}}(\vec{p}, \omega), \quad (\text{B2})$$

where, $\Gamma_{BCS} = \Gamma_{BCS}^A + \Gamma_{BCS}^R$ (2nd and 3rd terms in R.H.S of eq. B1) are mediated by advanced and retarded propagator of the photons and Γ_{fluct} (4th term) is mediated by the fluctuations of the photons. They take the form (see Eqs. 3 of the main text),

$$\begin{aligned}
\Gamma_{BCS}^{A(R)}(\vec{p}, \omega) &= \mathbf{i} \int \frac{d\vec{k}}{(2\pi)^2} \frac{d\omega_1}{2\pi} V^{(0)}(\vec{k} - \vec{p})D_{A(R)}(\omega_1 - \omega) G_{K(R)}(\vec{k}, \omega_1) G_{R(K)}(-\vec{k}, -\omega_1) \Gamma(\vec{k}, \omega_1) \\
\Gamma_{\text{fluct}}(\vec{p}, \omega) &= \mathbf{i} \int \frac{d\vec{k}}{(2\pi)^2} \frac{d\omega_1}{2\pi} V^{(0)}(\vec{k} - \vec{p})D_K(\omega_1 - \omega) G_R(\vec{k}, \omega_1) G_R(-\vec{k}, -\omega_1) \Gamma(\vec{k}, \omega_1). \quad (\text{B3})
\end{aligned}$$

To solve the BS equation for finding T_c , we first perform the integral over the loop momentum \vec{k} in Eq. B3 straightforwardly by using the delta-function structure of $V^{(0)}$ in the transferred momentum, $\vec{k} - \vec{p} = \pm \vec{q}_0$. Next, we do the integration over the

loop frequency ω_1 analytically either by using the the delta functions coming from G_K and D_K (see Eqs. A8 and A11) for the bare electrons and photons (in appendices C, D) or in case of broadened electrons and photons (in appendices E and F) by using the method of contour integration in complex frequency plane by computing residues at the simple poles of the electronic or photonic Green's function. This reduces the BS equation to an algebraic equation which couples the pairing amplitude $\Gamma_{\text{on-shell}}$ of the on-shell electrons ($\omega \sim \epsilon_{k_F \pm q_0}$) to that of the off-shell electrons far off from FS ($\omega \sim \pm \delta_c, \pm 2\delta_c, \dots$). In the next sections, we will discuss how to close this equation only in terms of the on-shell pairing amplitude $\Gamma_{\text{on-shell}}$ using the separation of electronic and photonic energy scales. Finally, the criterion of divergence of $\Gamma_{\text{on-shell}}$ in this equation will give us the critical temperature of the pairing instability.

In the next sections, we will discuss the BCS mechanism and the effect of photon fluctuations on the superconducting instability. In appendices C, D and E, we will restrict our discussion to the case of the closed system of 2D electrons coupled to the cavity where the total light-matter system is in thermal equilibrium. In appendices C and D, we will consider the electrons to be non-interacting while in appendix E, we will discuss effect of Coulomb (screened) repulsion between them in 2D. In appendix F, we will extend this discussion towards incorporating the effects of losses and incoherent pumping of the cavity.

Appendix C: BCS Pairing Mechanisms

In this section, we will evaluate the BCS terms, $\Gamma_{\text{BCS}}^{A(R)}$ (see Eq.B3) using the bare thermal Green's functions of the cavity photons (Eq. A11), the bare thermal electron Green's functions (Eq. A8) and the coupling function $V^{(0)}$. In the "BCS" terms, the spectral function of thermal electrons sets the internal frequency, $\omega_1 = \epsilon_k$, yielding,

$$\Gamma_{\text{BCS}}^A(\vec{p} = p\hat{x}, \omega) = \tilde{g}\delta_c \frac{\tanh\left(\frac{\epsilon_{p+q_0}}{2T}\right)}{\epsilon_{p+q_0}} \left[\Gamma(p+q_0, \epsilon_{p+q_0}) \left\{ 1 - \left(\frac{\epsilon_{p+q_0} - \omega}{\delta_c} \right)^2 \right\}^{-1} + \Gamma(p-q_0, \epsilon_{p-q_0}) \left\{ 1 - \left(\frac{\epsilon_{p-q_0} - \omega}{\delta_c} \right)^2 \right\}^{-1} \right], \quad (\text{C1})$$

where, $\tilde{g} = g_0^2/(4\pi\delta_c)^2$ is the dimensionless coupling constant. Setting the external momentum, $\vec{p} \sim k_F\hat{x}$ and the frequency, $\omega = \epsilon_{k_F \pm q_0}$, we can approximate $\Gamma(k_F \pm q_0, \epsilon_{k_F \pm q_0})$ in R.H.S by the pairing amplitude of the "on-shell" electrons for $q_0 \ll k_F$, i.e $\Gamma(k_F \pm q_0, \epsilon_{k_F \pm q_0}) \sim \Gamma_{\text{on-shell}}$. To gain a physical insight into the "BCS" mechanism, we further simplify the above equation by taking the adiabatic limit, where the frequency of the mediator photon, $\omega_1 - \omega = (\epsilon_{p \pm q_0} - \omega) \ll \delta_c$. In this limit, the above equation reduces to,

$$\Gamma_{\text{BCS}}^A(k_F\hat{x}, \epsilon_{k_F \pm q_0}) \sim 2\tilde{g}\delta_c \frac{\tanh\left(\frac{\epsilon_{p+q_0}}{2T}\right)}{\epsilon_{p+q_0}} \Gamma_{\text{on-shell}}. \quad (\text{C2})$$

The physical process behind the "BCS" pairing mechanism is explained in Fig. 1(c) of the main text. In this mechanism, an adiabatic photon scatters on-shell electron pair close to FS. Below the critical temperature, $T < T_c$, these low-energy electron pair form bound state, leading to divergence of pairing amplitude of on-shell electrons, $\Gamma_{\text{on-shell}}$. This gives an estimate of T_c , arising only from the standard BCS pairing mechanism, by equating the "BCS" part of Eq. B2, to $\Gamma(k_F\hat{x}, \epsilon_{k_F \pm q_0})$, i.e,

$$\begin{aligned} \Gamma(k_F\hat{x}, \epsilon_{k_F \pm q_0}) &= \Gamma_0 + \Gamma_{\text{BCS}}^A(k_F\hat{x}, \epsilon_{k_F \pm q_0}) + \Gamma_{\text{BCS}}^R(k_F\hat{x}, \epsilon_{k_F \pm q_0}) \\ &\Rightarrow \Gamma_{\text{on-shell}} = \Gamma_0 + 4\tilde{g}\delta_c \frac{\tanh\left(\frac{\epsilon_{k_F+q_0}}{2T_c}\right)}{\epsilon_{k_F+q_0}} \Gamma_{\text{on-shell}}. \end{aligned} \quad (\text{C3})$$

For divergence of the on-shell pairing amplitude $\Gamma_{\text{on-shell}}$ we have,

$$4\tilde{g}\delta_c \frac{\tanh\left(\frac{\epsilon_{k_F+q_0}}{2T_c}\right)}{\epsilon_{k_F+q_0}} = 1 \quad (\text{C4})$$

We numerically solve this equation to obtain T_c^{BCS} which is plotted as solid line with blue circles in Fig. 2(a) of the main text. Further, in the limit, $\epsilon_{k_F \pm q_0} \ll T$, we recover the polynomial dependence of the critical temperature on the coupling strength in Ref. 1,

$$T_c^{\text{BCS}} \sim 2\tilde{g}\delta_c, \quad (\text{C5})$$

for cavity-mediated long-range electron-electron interaction.

Appendix D: Fluctuation assisted enhancement of pairing instability

In this section, we will evaluate Γ_{fluct} (see Eq. B3) using the bare thermal Green's functions of the cavity photons (Eq. A11), the bare thermal electron Green's functions (Eq. A8) and the coupling function $V^{(0)}$. Γ_{fluct} is mediated by the Keldysh propagator of the photons and contains information about the spectral function of photons. The density of states of the thermal cavity photons set the internal frequency ω_1 close to the photon resonance frequency, i.e $\omega_1 = \pm\delta_c + \omega$. Hence, in this term, the mediator photons are the non-adiabatic photons with frequency $\omega_1 - \omega = \pm\delta_c$, which scatter the electrons far off the FS. This gives,

$$\Gamma_{\text{fluct}}(\vec{p} = k_F \hat{x}, \omega) \sim -2\tilde{g} \coth\left(\frac{\delta_c}{2T}\right) \left[\Gamma(k_F \hat{x} + q_0 \hat{x}, \omega + \delta_c) + \Gamma(k_F \hat{x} - q_0 \hat{x}, \omega + \delta_c) \right. \\ \left. + \Gamma(k_F \hat{x} + q_0 \hat{x}, \omega - \delta_c) + \Gamma(k_F \hat{x} - q_0 \hat{x}, \omega - \delta_c) \right], \quad (\text{D1})$$

where $\Gamma((k_F \pm q_0)\hat{x}, \omega \pm \delta_c)$ is the vertex function of the ‘‘off-shell’’ electron pair evaluated from, $\Gamma((k_F \pm q_0)\hat{x}, \omega \pm \delta_c) = \Gamma_0 + \Gamma_{\text{BCS}}((k_F \pm q_0)\hat{x}, \omega \pm \delta_c) + \Gamma_{\text{fluct}}((k_F \pm q_0)\hat{x}, \omega \pm \delta_c)$ (see Eq. B2). For large detuning δ_c compared to the on-shell electronic energies, the BCS contributions in the off-shell pairing amplitude at frequency $\omega \pm \delta_c$ cancel each other and the dominant contribution comes from the fluctuation term $\Gamma_{\text{fluct}}((k_F \pm q_0)\hat{x}, \omega + \delta_c) = \Gamma_{\text{fluct}}((k_F \pm q_0)\hat{x}, \omega - \delta_c)$.

Now, the ‘‘off-shell’’ vertex function has two contributions: (i) these ‘‘off-shell’’ electrons are subsequently scattered again by a non-adiabatic photons, which brings the electron-pair back close to the FS. This mechanism is depicted in Fig. 1(d) of the main text. This gives rise to an additional pairing mechanism between ‘‘on-shell’’ electrons, mediated by fluctuations of non-adiabatic photons, through virtual transition to ‘‘off-shell’’ electrons at the intermediate state of the process. Substituting the ‘‘on-shell’’ contribution coming from $\Gamma((k_F \pm q_0)\hat{x}, \omega \pm \delta_c)$, we get,

$$\Gamma_{\text{fluct}}(\vec{p} = k_F \hat{x}, \omega) = 16 (\tilde{g}\delta_c)^2 \coth\left(\frac{\delta_c}{2T}\right) \left[\frac{1}{\omega^2 - \epsilon_{k_F+2q_0}^2} + \frac{1}{\omega^2} \right] \Gamma_{\text{on-shell}}. \quad (\text{D2})$$

Setting $\omega = \epsilon_{k_F+q_0}$ as before and substituting Γ_{fluct} in Eq. B2, we obtain

$$\Gamma_{\text{on-shell}} = \Gamma_0 + \left[4\tilde{g}\delta_c \frac{\tanh\left(\frac{\epsilon_{k_F+q_0}}{2T_c^{\text{fluct}}}\right)}{\epsilon_{k_F+q_0}} + 16 (\tilde{g}\delta_c)^2 \coth\left(\frac{\delta_c}{2T_c^{\text{fluct}}}\right) \left\{ \frac{1}{\epsilon_{k_F+q_0}^2 - \epsilon_{k_F+2q_0}^2} + \frac{1}{\epsilon_{k_F+q_0}^2} \right\} \right] \Gamma_{\text{on-shell}}. \quad (\text{D3})$$

Here the first term within the parenthesis in R.H.S is coming from the standard BCS pairing mediated by the adiabatic photons while the second term comes from the new non-BCS pairing mediated by on-shell non-adiabatic photons.

The critical temperature, T_c^{fluct} of the 2D electrons incorporating both the BCS mechanism and fluctuation-assisted pairing by numerically solving the equation,

$$4\tilde{g}\delta_c \frac{\tanh\left(\frac{\epsilon_{k_F+q_0}}{2T_c^{\text{fluct}}}\right)}{\epsilon_{k_F+q_0}} + 16 (\tilde{g}\delta_c)^2 \coth\left(\frac{\delta_c}{2T_c^{\text{fluct}}}\right) \left[\frac{1}{\epsilon_{k_F+q_0}^2 - \epsilon_{k_F+2q_0}^2} + \frac{1}{\epsilon_{k_F+q_0}^2} \right] = 1 \quad (\text{D4})$$

We plot T_c^{fluct} by green dotted line in Fig. 2(a) of the main text. We can obtain a further simplified expression of T_c^{fluct} by approximating $\coth(\delta_c/(2T)) \sim 1$ at transition temperatures in the low Kelvin regime and $\epsilon_{k_F+2q_0}/\epsilon_{k_F+q_0} \sim 2$ using linearity of the electron dispersion close to the FS, given by,

$$T_c^{\text{fluct}} \sim 2\tilde{g}\delta_c \frac{1}{1 - \frac{32}{3}(\tilde{g}\delta_c)^2 \frac{1}{\epsilon_{k_F+q_0}^2}}. \quad (\text{D5})$$

This clearly shows that the fluctuation-assisted pairing term (second term of Eq. D4) modifies the corresponding BCS answer (Eq. C5) by decreasing the denominator significantly from 1. For realistic parameters of 2D materials (LAO/STO) coupled to a split-ring cavity¹⁻³, the ratio $\delta_c/\epsilon_{k_F+q_0} \sim 135$, and hence the the denominator is reduced from 1 already at moderate coupling strengths $\tilde{g} \sim 0.002$. Hence the additional pairing mechanism mediated by fluctuations of photons enhances the superconducting instability between the low-energy electrons, increasing T_c by order of magnitude.

(ii) Apart from the ‘‘on-shell’’ contribution of $\Gamma(k_F \pm q_0, \omega \pm \delta_c)$ discussed above, it has another contribution which connects to electrons farther off from FS at frequency $\omega \pm 2\delta_c$. These off-shell electrons can be scattered back close to FS via two types

of higher order scattering processes between on-shell and off-shell energy sector: (a) through Γ_{BCS} involving off-shell photons and (b) through Γ_{fluct} involving on-shell photons. The former process corrects Eq. D2 by powers of $\sim \tilde{g}\epsilon_{k_F \pm q_0}/\delta_c$, while the latter corrects it by powers of \tilde{g}^2 . These sub-leading corrections are suppressed as long as $\tilde{g}, \epsilon_{k_F \pm q_0}/\delta_c \ll 1$ and neglected for the present discussion.

At this point it is worthwhile to note that the coefficient of the fluctuation-assisted pairing term ($\propto 1/\epsilon_{k_F \pm q_0}^2$) is not regulated close to the FS and diverges in the limit $q_0 \rightarrow 0$. This is an artifact of using non-interacting (bare) electron Green's functions, without considering finite lifetime of the quasi-particles near FS. In the next section, we will take the Coulomb interaction between electrons in the 2D material into account. We will investigate the stabilization of enhancement mechanism by incorporating the fact that quasi-particles near the FS, which are taking part in the pairing mechanism, have only finite lifetime, dictated by Fermi-liquid nature of the 2D electron system.

Appendix E: Stabilization of the fluctuation-assisted enhancement

In the previous section, we discussed the effect of photon fluctuations in enhancing the pairing instability between the low energy electrons which were assumed to be non-interacting. In this section, we will incorporate the effects of Coulomb repulsion between the electrons within the scope of Fermi liquid theory⁹ of the 2D electron system. The screened Coulomb interaction potential induces the self-energy¹⁰ between the 2D electrons. The real part of the self-energy renormalizes the effective mass of the quasi-particles and the weight of the quasi-particle peak in the spectral function. However, for the present discussion of the 2D electrons, we will neglect these minor effects¹¹. At finite temperature, the dominant contribution is the broadening of the quasi-particle pole, coming from the imaginary part of the self-energy, leading to finite lifetime of the quasi-particles, given by¹⁰,

$$\begin{aligned} \frac{1}{\tau_{e,\text{cou}}(T; \epsilon_k)} &= \frac{\pi}{8} \frac{T^2}{E_F} \log\left(\frac{E_F}{T}\right), \text{ for } E_F \gg T \gg \epsilon_k \text{ and,} \\ &= \frac{\pi}{8} \frac{\epsilon_k^2}{E_F} \log\left(\frac{E_F}{\epsilon_k}\right), \text{ for } E_F \gg \epsilon_k \gg T \text{ and} \end{aligned} \quad (\text{E1})$$

Incorporating the quasi-particle lifetime, the bare Green's functions (Eq. A8) of the on-shell electrons will be modified to,

$$\begin{aligned} \mathcal{G}_{R(A)}(\vec{k}, \omega) &= \frac{1}{w - \epsilon_{\vec{k}} \pm i\tau_{e,\text{cou}}^{-1}(T; \epsilon_k)}, \\ \mathcal{G}_K(\vec{k}, \omega) &= \frac{1}{w - \epsilon_{\vec{k}} - i\tau_{e,\text{cou}}^{-1}} \frac{[-2i\tau_{e,\text{cou}}^{-1}(T; \epsilon_k) \tanh(\frac{\omega}{2T})]}{w - \epsilon_{\vec{k}} + i\tau_{e,\text{cou}}^{-1}}. \end{aligned} \quad (\text{E2})$$

We note that the Green's functions of the on-shell electrons dressed by the quasi-particle lifetime will be denoted by \mathcal{G} . On the other hand, the off-shell electrons having frequency close to the photon resonance frequency $\delta_c \gg \tau_{e,\text{cou}}^{-1}$ remain essentially unaffected by this correction and we will continue to use the bare Green's functions given in Eq. A8 for off-shell electrons. Using these Green's functions, we compute Γ_{BCS} and Γ_{fluct} and obtain $\Gamma_{\text{on-shell}}$ of the form,

$$\begin{aligned} \Gamma_{\text{on-shell}} &= \Gamma_0 + 4\tilde{g}\delta_c \text{Re} \left[\frac{\tanh\left(\frac{\epsilon_{k_F+q_0} - i\tau_{e,\text{cou}}^{-1}(T_c; \epsilon_{k_F+q_0})}{2T_c}\right)}{\epsilon_{k_F+q_0} - i\tau_{e,\text{cou}}^{-1}(T_c; \epsilon_{k_F+q_0})} \right] \Gamma_{\text{on-shell}} + \\ &16(\tilde{g}\delta_c)^2 \coth\left(\frac{\delta_c}{2T_c}\right)^2 \text{Re} \left[\frac{1}{\epsilon_{k_F+q_0}^2 - \{\epsilon_{k_F+2q_0} - i\tau_{e,\text{cou}}^{-1}(T_c; \epsilon_{k_F+2q_0})\}^2} + \frac{1}{\epsilon_{k_F+q_0}^2 + \tau_{e,\text{cou}}^{-2}(T_c; 0)} \right] \Gamma_{\text{on-shell}} \end{aligned} \quad (\text{E3})$$

Here, the 2nd term in R.H.S corresponds to the BCS contribution while the 3rd term corresponds to the fluctuation-assisted pairing term. Note that the finite lifetime of electrons induce leading temperature dependence in the fluctuation-assisted pairing term, while the BCS term is not affected by this correction in leading order due to smoothening of the Fermi-Dirac distribution. A numerical estimate of T_c is obtained by solving the BS equation for the divergence of the on-shell pairing amplitude from the

equation,

$$4\tilde{g}\delta_c \text{Re} \left[\frac{\tanh\left(\frac{\epsilon_{k_F+q_0} - i\tau_{e,\text{cou}}^{-1}(T_c; \epsilon_{k_F+q_0})}{2T_c}\right)}{\epsilon_{k_F+q_0} - i\tau_{e,\text{cou}}^{-1}(T_c; \epsilon_{k_F+q_0})} \right] + 16(\tilde{g}\delta_c)^2 \coth\left(\frac{\delta_c}{2T_c}\right)^2 \text{Re} \left[\frac{1}{\epsilon_{k_F+q_0}^2 - \{\epsilon_{k_F+2q_0} - i\tau_{e,\text{cou}}^{-1}(T_c; \epsilon_{k_F+2q_0})\}^2} + \frac{1}{\epsilon_{k_F+q_0}^2 + \tau_{e,\text{cou}}^{-2}(T_c; 0)} \right] = 1. \quad (\text{E4})$$

We plot this numerical answer of T_c as a solid line (magenta) in Fig. 2(a) in the main text. At low temperatures $\tau_{e,\text{cou}}^{-1}(T; \epsilon_k) \ll \epsilon_k$ at $k = k_F \pm q_0, k_F \pm 2q_0$ and this answer closely matches with T_c^{fluct} . This figure also clearly indicates that photon fluctuations lead to a significant enhancement of T_c , from the BCS answer over the entire range of \tilde{g} plotted in Fig. 2(a) of the main text. In high temperature limit, the quasi-particle broadening energy scale, $\tau_{e,\text{cou}}^{-1}$, dominates over the typical energy of ‘‘on-shell’’ electrons, i.e $\tau_{e,\text{cou}}^{-1}(T; \epsilon_k) \gg \epsilon_k$ at $k = k_F \pm q_0, k_F \pm 2q_0$. In this limit, we obtain an estimate of the critical temperature, T_c^{high} by solving the equation,

$$4\tilde{g}\delta_c \text{Re} \left[\frac{\tanh\left(\frac{-i\tau_{e,\text{cou}}^{-1}(T_c^{\text{high}}; 0)}{2T_c^{\text{high}}}\right)}{-i\tau_{e,\text{cou}}^{-1}(T_c^{\text{high}}; 0)} \right] + 32(\tilde{g}\delta_c)^2 \coth\left(\frac{\delta_c}{2T_c^{\text{high}}}\right)^2 \frac{1}{\tau_{e,\text{cou}}^{-2}(T_c^{\text{high}}; 0)} = 1, \quad (\text{E5})$$

A simplified form the above equation, obtained by smoothening the Fermi-Dirac distribution in the BCS term, is given in Eq. 8 of the main text. In the high temperature limit, T_c^{high} (dashed line in Fig. 2(a)) shows good agreement with the full numerical answer.

To this end, it is instructive to note that the effective interaction between the on-shell (low-energy) electrons is attractive if the effective coupling function, $\Gamma_{\text{on-shell}}$ between the on-shell electrons is negative. Since in Eq. E3 $\Gamma_0 < 0$ and the coefficient of the BCS term is positive, the criterion $\Gamma_{\text{on-shell}} < 0$ will be trivially ensured when the coefficient of the non-BCS pairing is also positive. In this case, the new non-BCS mechanism will contribute favorably to the attractive pairing. At low T ($\tau_{e,\text{cou}}^{-1}(T; \epsilon_k) \ll \epsilon_k$), Eq. E3 reduces to Eq. D3 which imposes the condition, $\epsilon_{k_F+2q_0} > \sqrt{2}\omega$ for the effective interaction to be attractive. For our particular case, $\omega = \epsilon_{k_F+q_0}$. Assuming a linear dispersion close to FS, we get $\epsilon_{k_F+2q_0} = 2\epsilon_{k_F+q_0}$ and hence the above criterion is satisfied. On the other hand, at large T ($\tau_{e,\text{cou}}^{-1}(T; \epsilon_k) \gg \epsilon_k$), the coefficient of the non-BCS pairing, governed only by the broadening of the quasi-particles, is always positive and hence contribute favorably to the attractive pairing.

Appendix F: Role of cavity loss and incoherent pump

In the previous sections, we considered the coupled light-matter system to be a closed system which is in thermal equilibrium at temperature, T . In this section, we will extend this analysis to the case of an open system with a driven-dissipative cavity. We will investigate the effects of the leakage of photons from the cavity as well as incoherent pumping of photons into the cavity. In presence of single-particle loss of photons at a rate γ_{loss} and incoherent single-particle pump of photons at a rate γ_{pump} , the dynamics of the cavity photons is described by the non-equilibrium Markovian master equation for the density matrix $\hat{\rho}(t)$ ^{12,13},

$$\partial_t \hat{\rho} = -\mathbf{i}[H_c, \hat{\rho}] + \gamma_{\text{pump}} \left(b^\dagger \hat{\rho} b - \frac{1}{2} \{bb^\dagger, \hat{\rho}\} \right) + \gamma_{\text{loss}} \left(b \hat{\rho} b^\dagger - \frac{1}{2} \{b^\dagger b, \hat{\rho}\} \right), \quad (\text{F1})$$

where the first term in R.H.S generates the coherent dynamics by the cavity Hamiltonian H_c (see eq.A2). The validity of the Markovian description lies in the fact the cavity photons are driven by the external laser of frequency ω_L which is much larger than other frequency scales, i.e $\omega_L \gg \delta_c \gg \epsilon_{k_F+q_0}$. Hence, the dynamics in the rotating frame can be described very well by neglecting the memory effects in the dissipative and noise kernel induced by the external vacuum field. We convert the above master equation into an equivalent description in terms of Keldysh path integral¹³ and the bare Green’s functions of the cavity photons (see eq.A11) are modified to,

$$D_{R(A)}(\omega) = \frac{1}{2} \frac{1}{(\omega \pm i\kappa^+)^2 - \delta_c^2}, \quad D_K(\omega) = -\mathbf{i} \frac{\gamma}{\delta_c} \frac{\omega^2 + \kappa^2 + \delta_c^2}{(\omega^2 - \kappa^2 - \delta_c^2)^2 + 4\kappa^2\omega^2}. \quad (\text{F2})$$

Here, $\kappa = (\gamma_{\text{loss}} - \gamma_{\text{pump}})/2$ is the net decay rate (inverse lifetime) of the cavity photons and $\gamma = (\gamma_{\text{loss}} + \gamma_{\text{pump}})/2 > \kappa$ defines the total noise level. In this case, the inelastic scattering between the electrons and the cavity photons further reduces the lifetime of the quasi-particles (in addition to the Coulomb lifetime) which we take into account by calculating the Fock-diagrams⁴ for

the cavity induced self-energies,

$$\begin{aligned}\Sigma_{R,\text{cav}}(\omega, \vec{p}) &= \frac{\mathbf{i}}{2} \int \frac{d\vec{k}}{(2\pi)^2} \int \frac{d\omega_1}{2\pi} V^{(0)}(\vec{p} - \vec{k}) \left[D_R(\omega - \omega_1) G_K(\omega_1, \vec{k}) + D_K(\omega - \omega_1) G_R(\omega_1, \vec{k}) \right] \\ \Sigma_{K,\text{cav}}(\omega, \vec{p}) &= \frac{\mathbf{i}}{2} \int \frac{d\vec{k}}{(2\pi)^2} \int \frac{d\omega_1}{2\pi} V^{(0)}(\vec{p} - \vec{k}) \left[D_R(\omega - \omega_1) G_R(\omega_1, \vec{k}) + D_A(\omega - \omega_1) G_A(\omega_1, \vec{k}) \right. \\ &\quad \left. + D_K(\omega - \omega_1) G_K(\omega_1, \vec{k}) \right]\end{aligned}\quad (\text{F3})$$

We use the bare electron Green's functions given in eq. A8 and the driven-dissipative photonic Green's functions given in eq. F2 to compute the self-energies. In the leading order approximation of $\delta_c \gg \epsilon_{k_F \pm q_0}$, $\text{Im}[\Sigma_{R,\text{cav}}(\omega, \vec{p})] \simeq -2\tilde{g}\gamma/(1 + \kappa^2/\delta_c^2)$ and $\Sigma_{K,\text{cav}}(\omega, \vec{p}) \simeq -2\mathbf{i}\tilde{g}\gamma/(1 + \kappa^2/\delta_c^2) \{ \tanh(\epsilon_{p+q_0}/(2T)) + \tanh(\epsilon_{p-q_0}/(2T)) \}$. This modifies the total inverse lifetime of the quasi-particles as, $\tau_e^{-1} = \tau_{e,\text{cou}}^{-1} + \tau_{e,\text{cav}}^{-1}$, with $\tau_{e,\text{cav}}^{-1} \simeq 2\tilde{g}\gamma/(1 + \kappa^2/\delta_c^2)$. The Green's functions of the on-shell electrons (see eq. E2) are modified as,

$$\begin{aligned}\mathcal{G}_{R(A)}(\vec{k}, \omega) &= \frac{1}{w - \epsilon_{\vec{k}} \pm \mathbf{i}\tau_e^{-1}(T; \epsilon_k)}, \\ \mathcal{G}_K(\vec{k}, \omega) &= \frac{1}{w - \epsilon_{\vec{k}} - \mathbf{i}\tau_e^{-1}} \frac{[-2\mathbf{i}\tau_e^{-1}(T; \epsilon_k) \tanh(\frac{\omega}{2T})]}{w - \epsilon_{\vec{k}} + \mathbf{i}\tau_e^{-1}},\end{aligned}\quad (\text{F4})$$

while the Green's functions for the off-shell electrons essentially remain unaffected and are given by the bare electronic Green's functions in eq. A8.

We will now calculate the BCS and the fluctuation (noise) terms of the BS equation (Eqs. B3) using the dissipative photonic Green's functions (F2), dressed Green's functions for the on-shell electrons (F4) and the bare Green's functions for the off-shell electrons (A8). This modifies the BCS contribution Γ_{BCS} given in eq. C1 to,

$$\begin{aligned}\Gamma_{BCS}^{A(R)}(\vec{p} = p\hat{x}, \omega) &= \tilde{g}\delta_c \frac{\tanh(\frac{\epsilon_{p+q_0}}{2T})}{\epsilon_{p+q_0}} \left[\left\{ 1 - \left(\frac{\epsilon_{p+q_0} \mp \omega - \mathbf{i}(\kappa + \tau_e^{-1})}{\delta_c} \right)^2 \right\}^{-1} \right. \\ &\quad \left. + \left\{ 1 - \left(\frac{\epsilon_{p-q_0} \mp \omega - \mathbf{i}(\kappa + \tau_e^{-1})}{\delta_c} \right)^2 \right\}^{-1} \right] \Gamma_{\text{on-shell}},\end{aligned}\quad (\text{F5})$$

Setting $p = k_F$ and $\omega = \epsilon_{k_F \pm q_0}$ as before, we solve the BS equation taking contributions only from the BCS terms, i.e. $\Gamma_{\text{on-shell}} = \Gamma_0 + [\Gamma_{BCS}^A(k_F\hat{x}, \epsilon_{k_F+q_0}) + \Gamma_{BCS}^A(k_F\hat{x}, \epsilon_{k_F-q_0}) + \Gamma_{BCS}^R(k_F\hat{x}, \epsilon_{k_F+q_0}) + \Gamma_{BCS}^R(k_F\hat{x}, \epsilon_{k_F-q_0})]/2$ for a divergent on-shell pairing amplitude. This gives the numerical estimate of T_c^{BCS} plotted in Fig. 2(b) of the main text by solid line with circles in the case of driven-dissipative photons. The facts that the laser detuning δ_c is much larger compared to the on-shell electronic scales and the quasi-particles are long-lived compared to cavity photons at low temperatures (T_c^{BCS} ranging from 0.01K to 0.1K), further simplify the equation for T_c^{BCS} to,

$$T_c^{\text{BCS}} \simeq 2\tilde{g}\delta_c \frac{1}{1 + \frac{\kappa^2}{\delta_c^2}}.\quad (\text{F6})$$

This shows the BCS prediction for critical temperature remains essentially unaffected by cavity losses ($\kappa \ll \delta_c$) and independent of the incoherent pumping of photons into the cavity.

We now calculate the fluctuation term Γ_{fluct} in the BS equation (eq. (3) of the main text). In the case of the driven-dissipative cavity, the distribution function of the cavity photons is no longer sharp delta functions at the cavity resonance frequencies ($\pm\delta_c$), rather broadened by the finite cavity lifetime. In this case, Γ_{fluct} has contributions coming from two terms: $\Gamma_{\text{fluct}} = \Gamma_{\text{fluct}}^{\text{photon}} + \Gamma_{\text{fluct}}^{\text{electron}}$ where $\Gamma_{\text{fluct}}^{\text{electron}}$ is the contribution when we choose the pole of the on-shell electronic Green's functions which sets the internal frequency $\omega_1 = \epsilon_k - \mathbf{i}\tau_e^{-1}$, while $\Gamma_{\text{fluct}}^{\text{photon}}$ is the one when we choose the poles of the photonic Green's

functions which sets $\omega_1 = \pm\delta_c - \mathbf{i}\kappa + \omega$ (see Eq.B3). This modifies eq. D1 to yield the fluctuation contributions,

$$\begin{aligned} \Gamma_{\text{fluct}}^{\text{photon}}(\vec{p} = k_F \hat{x}, \omega) &= \tilde{g} \delta_c^2 \frac{\gamma}{\kappa} \sum_{\vec{k}=(k_F \pm q_0) \hat{x}} \left[G_R(\vec{k}, \omega + \delta_c - \mathbf{i}\kappa) G_R(-\vec{k}, -(\omega + \delta_c - \mathbf{i}\kappa)) \Gamma(\vec{k}, \omega + \delta_c - \mathbf{i}\kappa) \right. \\ &\quad \left. + G_R(\vec{k}, \omega - \delta_c - \mathbf{i}\kappa) G_R(-\vec{k}, -(\omega - \delta_c - \mathbf{i}\kappa)) \Gamma(\vec{k}, \omega - \delta_c - \mathbf{i}\kappa) \right], \\ \Gamma_{\text{fluct}}^{\text{electron}}(\vec{p} = k_F \hat{x}, \omega) &= 2\mathbf{i} \tilde{g} \delta_c^2 \gamma \sum_{\vec{k}=(k_F \pm q_0) \hat{x}} \frac{\left[(\epsilon_k - \omega - \mathbf{i}\tau_e^{-1})^2 + \kappa^2 + \delta_c^2 \right] \Gamma_{\text{on-shell}}}{\left[(\epsilon_k - \omega - \mathbf{i}(\tau_e^{-1} + \kappa))^2 - \delta_c^2 \right] \left[(\epsilon_k - \omega - \mathbf{i}(\tau_e^{-1} - \kappa))^2 - \delta_c^2 \right] \left[\epsilon_k - \mathbf{i}\tau_e^{-1} \right]}, \end{aligned} \quad (\text{F7})$$

where $\Gamma((k_F \pm q_0) \hat{x}, \omega \pm \delta_c - \mathbf{i}\kappa)$ is evaluated from, $\Gamma((k_F \pm q_0) \hat{x}, \omega \pm \delta_c - \mathbf{i}\kappa) = \Gamma_0 + \Gamma_{\text{BCS}}((k_F \pm q_0) \hat{x}, \omega \pm \delta_c - \mathbf{i}\kappa) + \Gamma_{\text{fluct}}((k_F \pm q_0) \hat{x}, \omega \pm \delta_c - \mathbf{i}\kappa)$ (see Eq. B2). As we discussed in appendix D, we will calculate the contribution of $\Gamma((k_F \pm q_0) \hat{x}, \omega \pm \delta_c - \mathbf{i}\kappa)$ to the on-shell pairing amplitude and substitute in $\Gamma_{\text{fluct}}^{\text{photon}}$ which will close the BS equation in frequency space. We can compute each term of $\Gamma((k_F \pm q_0) \hat{x}, \omega \pm \delta_c - \mathbf{i}\kappa)$ from,

$$\begin{aligned} \Gamma_{\text{BCS}}^A(\vec{p} = p \hat{x}, \omega \pm \delta_c - \mathbf{i}\kappa) &= -\tilde{g} \delta_c^2 \sum_{\vec{k}=\vec{p} \pm q_0 \hat{x}} \left[\frac{\pm 1}{2} \mathcal{G}_K(\vec{k}, \omega) \mathcal{G}_R(-\vec{k}, -\omega) \right. \\ &\quad \left. + \tanh \frac{\epsilon_k - \mathbf{i}\tau_e^{-1}}{2T} \frac{\delta_c}{\epsilon_k - \mathbf{i}\tau_e^{-1}} \frac{1}{(\epsilon_k - \omega \mp 2\delta_c - \mathbf{i}\tau_e^{-1}) (\epsilon_k - \omega - \mathbf{i}\tau_e^{-1})} \right] \Gamma_{\text{on-shell}} \\ \Gamma_{\text{BCS}}^R(\vec{p} = p \hat{x}, \omega \pm \delta_c - \mathbf{i}\kappa) &= -\tilde{g} \delta_c^3 \sum_{\vec{k}=\vec{p} \pm q_0 \hat{x}} \left[\frac{\tanh \frac{\epsilon_k - \mathbf{i}\tau_e^{-1}}{2T}}{\epsilon_k - \mathbf{i}\tau_e^{-1}} \frac{\Gamma_{\text{on-shell}}}{(\epsilon_k + \omega \pm 2\delta_c - \mathbf{i}(\tau_e^{-1} + 2\kappa)) (\epsilon_k + \omega - \mathbf{i}(\tau_e^{-1} + 2\kappa))} \right] \\ \Gamma_{\text{fluct}}(\vec{p} = p \hat{x}, \omega \pm \delta_c - \mathbf{i}\kappa) &= \tilde{g} \delta_c^2 \sum_{\vec{k}=\vec{p} \pm q_0 \hat{x}} \left[\frac{\gamma}{2\kappa} \mathcal{G}_R(\vec{k}, \omega) \mathcal{G}_R(-\vec{k}, -\omega) \right. \\ &\quad \left. - 4\mathbf{i}\gamma \tilde{D}_K(-\epsilon_k + \mathbf{i}\tau_e^{-1} - (\omega \pm \delta_c - \mathbf{i}\kappa)) \mathcal{G}_R(-\vec{k}, -\epsilon_k + \mathbf{i}\tau_e^{-1}) \right] \Gamma_{\text{on-shell}}, \end{aligned} \quad (\text{F8})$$

where, $\tilde{D}_K(\omega) = (\omega^2 + \kappa^2 + \delta_c^2) / [\{(\omega - \mathbf{i}\kappa)^2 - \delta_c^2\} \{(\omega + \mathbf{i}\kappa)^2 - \delta_c^2\}]$. Using the above equations and setting $p = k_F$ and $\omega = \epsilon_{k_F \pm q_0}$, we obtain $\Gamma_{\text{fluct}}^{\text{photon}}$ and hence Γ_{fluct} in terms of $\Gamma_{\text{on-shell}}$. Substituting in eq.B2, we solve the BS equation for the divergent on-shell pairing amplitude. This gives a numerical estimate of T_c^{noise} which is plotted in Fig. 2(b) of the main text. Following arguments similar to the ones given in appendix D, one can show that the dominant contribution in $\Gamma((k_F \pm q_0) \hat{x}, \omega \pm \delta_c - \mathbf{i}\kappa)$ will come from $\Gamma_{\text{fluct}}((k_F \pm q_0) \hat{x}, \omega \pm \delta_c - \mathbf{i}\kappa)$ in the limit of large detuning δ_c compared to the electronic scales and κ . Moreover, for $\tilde{g} \delta_c^2 / \kappa^2 \gg 1$, $\Gamma_{\text{fluct}}^{\text{photon}}$ dominates over $\Gamma_{\text{fluct}}^{\text{electron}}$. In this limit, at high temperatures where the quasi-particle broadening $\tau_e^{-1} \gg \epsilon_{k_F \pm q_0}$, a simplified expression for T_c^{noise} is given in eq. (11) of the main text.

* ahana@pks.mpg.de

† piazza@pks.mpg.de

¹ H. Gao, F. Schlawin, M. Buzzi, A. Cavalleri, and D. Jaksch, *Phys. Rev. Lett.* **125**, 053602 (2020).

² T. Sakudo and H. Unoki, *Phys. Rev. Lett.* **26**, 851 (1971).

³ X. Lin, Z. Zhu, B. Fauqué, and K. Behnia, *Phys. Rev. X* **3**, 021002 (2013).

⁴ A. Kamenev, *Field theory of non-equilibrium systems* (Cambridge University Press, 2011).

⁵ J. W. Negele and H. Orland, *Quantum Many Body Systems* (Oxford University Press on Demand, 2002).

⁶ A. Altland and B. D. Simons, *Condensed matter field theory* (Cambridge University Press, 2010).

⁷ A. A. Abrikosov, I. Dzyaloshinskii, L. P. Gorkov, and R. A. Silverman, *Methods of quantum field theory in statistical physics* (Dover, New York, NY, 1975).

⁸ R. D. Mattuck, *Methods of Quantum Field Theory in Statistical Physics* (Dover Publications, INC. New York, 1992).

⁹ D. Pines and P. Nozières, *The theory of quantum liquids normal fermi liquids* (2018) pp. 1–180.

¹⁰ L. Zheng and S. Das Sarma, *Phys. Rev. B* **53**, 9964 (1996).

¹¹ T. Jungwirth and A. H. MacDonald, *Phys. Rev. B* **53**, 7403 (1996).

- ¹² E. G. D. Torre, S. Diehl, M. D. Lukin, S. Sachdev, and P. Strack, *Phys. Rev. A* **87**, 023831 (2013).
- ¹³ L. M. Sieberer, M. Buchhold, and S. Diehl, *Reports on Progress in Physics* **79**, 096001 (2016).